

# Lagged couplings diagnose Markov chain Monte Carlo phylogenetic inference

Luke J. Kelly\*, Robin J. Ryder\* and Grégoire Clarté\*

**Abstract.** Phylogenetic inference is an intractable statistical problem on a complex sample space. Markov chain Monte Carlo methods are the primary tool for Bayesian phylogenetic inference, but it is challenging to construct efficient schemes to explore the associated posterior distribution and to then assess their convergence. Building on recent work developing couplings of Monte Carlo algorithms, we describe a procedure to couple Markov Chains targeting a posterior distribution over a space of phylogenetic trees with ages, scalar parameters and latent variables. We demonstrate how to use these couplings to check convergence and mixing time of the chains.

**MSC2020 subject classifications:** Primary 65C05, 60K35; secondary 62F15, 92D15.

**Keywords:** MCMC methods, Couplings, Bayesian phylogenetics.

## 1 Introduction

Phylogenetic inference is the problem of reconstructing the ancestral history of a set of taxa descended from a common ancestor. The phylogeny is typically represented by a bifurcating tree, where the external leaf nodes correspond to observed taxa and unobserved internal nodes to speciation events. There are many tools for performing model-based Bayesian phylogenetic inference, including **MrBayes** (Ronquist et al., 2012), **RevBayes** (Höhna et al., 2016), **BEAST** (Bouckaert et al., 2019), and **Blang** (Bouchard-Côté et al., 2021), and these methods are routinely applied in fields ranging from the life sciences (McPherson et al., 2016; Morel et al., 2020; Lemey et al., 2021) to humanities (Watts et al., 2016; Greenhill et al., 2017; Sagart et al., 2019).

Phylogenetic inference is an intractable problem (Willis and Bell, 2018; Willis, 2019) as we attempt to infer a complex, high-dimensional object on a general state space with many latent variables and an often multimodal likelihood function. When calculating the likelihood in a phylogenetic model, we attempt to integrate out as many latent variables as possible; although the likelihood can often be computed efficiently (Felsenstein, 1981) with cost that grows linearly with the number of taxa, there are models where the computational cost grows exponentially in the number of taxa (Kelly and Nicholls, 2017).

Many modern phylogenetic methods specify a generative model for the data: a branching process on species defines the tree, and a diversification process acting on sequences of complex evolutionary traits represents the evolution of the species along the tree. We

---

\*CEREMADE, CNRS, UMR 7534, Université Paris-Dauphine, PSL University, 75016 Paris, France  
[kelly@ceremade.dauphine.fr](mailto:kelly@ceremade.dauphine.fr); [ryder@ceremade.dauphine.fr](mailto:ryder@ceremade.dauphine.fr); [clarte@ceremade.dauphine.fr](mailto:clarte@ceremade.dauphine.fr)

can place priors on the tree and model parameters and perform inference by drawing samples from the posterior. Markov chain Monte Carlo (MCMC) is the primary tool for performing Bayesian phylogenetic inference via the Metropolis–Hastings algorithm (Hastings, 1970) and is the focus of our paper. Constructing a chain which explores the posterior in a reasonable amount of time is a difficult problem and an active area of research (Whidden et al., 2019) and many leading Bayesian phylogenetic software packages implement adaptive Monte Carlo schemes (Ronquist et al., 2012; Höhna et al., 2016; Bouckaert et al., 2019). In certain classes of problems, we can use piecewise-deterministic Markov processes (Zhang et al., 2021; Koskela, 2020), sequential Monte Carlo (Wang et al., 2019), Hamiltonian Monte Carlo (Bastide et al., forthcoming) or variational approximations (Zhang and Matsen IV, 2019). In any case, we lack methods to properly quantify convergence or mixing of Markov schemes on the space of trees and model parameters so struggle to separate modelling and fitting errors (Fourment et al., 2019).

Phylogenetic inference is computationally expensive so we desire not only to check convergence, but also to discover convergence shortly after it occurs to avoid wasting the output. As data sets increase in size, practitioners resort to running ever longer chains from different initial configurations (Whidden and Matsen IV, 2015) to see whether they converge to similar distributions at a similar rate, but the methods for assessing this are ad hoc as we struggle to compare joint distributions on trees and model parameters. Furthermore, we lack tools to remove potential bias in estimators with respect to the posterior distribution which would allow us to safely and efficiently combine estimates from multiple independent chains.

In a recent series of important papers, Pierre Jacob and collaborators have developed techniques using couplings to construct unbiased estimators and derive bounds on the convergence of MCMC chains on general state spaces. Jacob et al. (2020) construct two Markov chains  $(X_t)$  and  $(Y_t)$  with common stationary distribution  $\pi$  and transition kernel  $P$  on space  $\mathcal{X}$ , such that the lag-1 staggered chains  $(X_t)$  and  $(Y_{t-1})$  meet at a random, finite time  $\tau$  and remain coupled thereafter. Provided that the tails of the meeting time distribution are at most geometric, we can debias finite-sample Monte Carlo estimators of  $\int_{\mathcal{X}} f(X) d\pi(X)$  for any integrable function  $f$ . We can then safely average estimators from multiple pairs of chains run in parallel. In subsequent work, Heng and Jacob (2019) develop couplings of Hamiltonian Monte Carlo transition kernels and Middleton et al. (2020) allow for polynomial tails of the meeting time distribution.

Including the initial samples before the Markov chains have reached convergence increases the variance of the unbiased estimators, so we would like to discard the samples before convergence as *burn-in*. By coupling chains at lag  $l > 1$ , Biswas et al. (2019) bound integral probability metrics such as the total variation (TV) distance between  $\pi_t$ , the marginal distribution of  $X_t$ , and the target  $\pi$  by

$$d_{\text{TV}}(\pi_t, \pi) \leq \mathbb{E} \left[ 0 \vee \left\lceil \frac{\tau - l - t}{l} \right\rceil \right]. \quad (1)$$

The expectation in Equation 1 is with respect to the distribution of  $\tau$  so can be estimated with the coupling times from multiple independent pairs of chains. The TV bound

becomes sharper as the lag  $l$  increases so in practice we repeat the experiment for a grid of lag values until the estimated bound stabilises. Slow mixing between modes manifests as plateaus in the bound as pairs of chains in different modes struggle to meet; initialising pairs of chains further apart typically increases the coupling time but reduces its variance so produces more useful bounds. In pursuing this approach, we can objectively diagnose convergence jointly on all of the parameters with a meaningful metric. In addition, we can construct unbiased estimators from the samples which can be averaged across chains.

In order to implement these methods to be useful in practice, we require a coupling which has a positive probability that the chains will meet on at least some regions of the state space. Previous efforts have focused on situations where the state space has a straightforward geometry, typically a subset of  $\mathbb{R}^d$  (Bou-Rabee and Eberle, 2020; Biswas et al., 2020), or problems such as the Ising model (Jacob et al., 2020). In this paper, we describe techniques to couple Markov chains exploring a posterior distribution over a space of phylogenetic trees and model parameters to so that we can produce a useful bound on the total variation distance for diagnosing convergence and construct unbiased estimators. Note that this framework is very different to what has also been called *coupled MCMC for phylogenies* in other works, such as Müller and Bouckaert (2020) who consider parallel tempering to explore the posterior distribution.

This extension to phylogenetic problems is not straightforward for a number of reasons. As we describe above, phylogenetic models are intractable functions on general state spaces with complex geometry (Billera et al., 2001). Theoretical analyses of Markov chains in phylogenetic inference are restricted to special cases (Aldous, 2000; Mossel and Vigoda, 2006). Phylogenetic posterior distributions are frequently multi-modal (Whidden and Matsen IV, 2015; Whidden et al., 2019), and in addition the model often imposes constraints on the possible trees while each tree topology constrains the possible branch lengths. MCMC proposal distributions which update the entire phylogenetic state or large portions of it are intractable as we cannot compute easily the density of a transition kernel which targets efficiently the entire state space; in practice, we can only propose local, componentwise modifications to the current state. Our MCMC transition kernel is thus a mixture of several kernels, each proposing modifications to some local aspect of the state.

In attempting to couple chains, the region of space where we can make an identical proposal to both states is extremely small and requires the states to already be identical in many respects. To obtain a successful coupling from arbitrary starting points, we therefore require the chains to come sufficiently close that we can couple them piece-by-piece. In order to do so, we must make proposals to both chains which make the states increasingly similar, until a coupling of the whole state becomes possible. As a benefit of attempting to couple chains, we can identify moves to add to our proposal kernel from chains which fail to couple.

The remainder of this paper is arranged as follows. In Section 2, we introduce the problem of Bayesian phylogenetic inference via Markov chain Monte Carlo methods and describe existing methods for assessing convergence in this setting. Section 3 describes how to construct couplings of MCMC transition kernels for phylogenetic models and



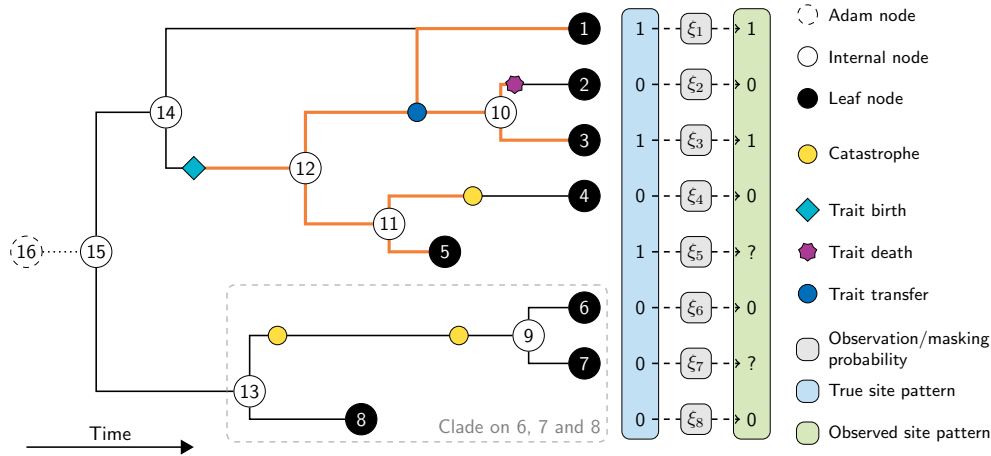


Figure 2: A trait history (orange) drawn from the Stochastic Dollo model on a phylogenetic tree. The trait is born near the root and survives to be present in leaves 1, 3 and 5, but as a result of a masking process is only observed at leaves 1 and 3. Catastrophes advance the trait process on their branch through an instantaneous burst of evolutionary activity. A clade constraint identifies taxa 6, 7, and 8 as forming a subtree of the phylogeny.

species at a speciation event; instances of each trait die independently at rate  $\mu$ . We record the pattern of presence or absence displayed by each trait across the leaves. In addition, we may allow for bursts of evolutionary in the form of a Poisson process at rate  $\rho$  of catastrophes with strength  $\kappa$  along the tree (Ryder and Nicholls, 2011), and instances of traits attempt to transfer copies of themselves into other branches at rate  $\beta$  (Kelly and Nicholls, 2017). Under the Dollo parsimony assumption, a trait may only arise once on the tree and once extinct remains so. As we have a Poisson process of new traits with independent thinning, the number of traits at the leaves displaying each binary pattern of presence/absence is Poisson; we can calculate the rate parameters by integrating over the unobserved trait events on the tree. Figure 2 illustrates the SD model, we present a more detailed discussion in Appendix A.

## 2.2 Bayesian inference in phylogenetic models

Phylogenetic inference is difficult for a number of reasons. The parameters of a phylogenetic model are on a general state space with complex dependencies between them. The tree topology is discrete and the number of possible tree topologies grows exponentially in the number of taxa. Each topology induces a partial ordering on possible internal node times; leaf nodes are typically fixed to age 0. In the SD model, catastrophes are indexed by their branch and relative position along it: they thus provide an example of a set of latent variables attached to each branch, which is a feature found in many other models. Phylogenetic posterior distributions are often multimodal (Beiko et al., 2006; Whidden and Matsen IV, 2015; Whidden et al., 2019), and model parameters are often

highly dependent on the tree and vice versa. The SD model rate parameters and tree node times are not identifiable without constraints on the model so, where available, we incorporate expert prior information on the tree through *clade* constraints. Each clade asserts that a set of taxa form a subtree or specifies a time interval for their most recent common ancestor; Figure 2 includes an example of a clade.

In this paper, we focus on Markov chain Monte Carlo (MCMC) approaches to inference: we construct an ergodic Markov chain  $(X_t)_t$  with transition kernel  $P$  that leaves the posterior distribution  $\pi$  invariant. At each iteration  $t$ , we sample the new state  $X_t \sim P(X_{t-1}, \cdot)$  via the Metropolis–Hastings (MH) algorithm. We denote  $Q$  our proposal distribution, and for a pair of states  $X$  and  $X'$  define the acceptance probability  $\alpha(X, X') = \min[1, \pi(X')Q(X', X)/\pi(X)Q(X, X')]$ . The Metropolis–Hastings algorithm proceeds as follows at iteration  $t$ :

1. Sample proposal  $X' \sim Q(X_{t-1}, \cdot)$
2. Sample acceptance indicator  $B \sim \text{Bern}(\alpha(X_{t-1}, X'))$
3. Set  $X_t = BX' + (1 - B)X_{t-1}$ .

Proposals which update the entire phylogenetic state  $X$  are intractable as we cannot easily compute neighbourhoods or proposal densities except for relatively simple moves. For example, although the space of topologies is finite, exploring it efficiently is difficult; in practice, we rely on local moves such as the SPR move defined below, but computing SPR neighbourhood sets of the current state is computationally expensive (Song, 2003; Whidden and Matsen IV, 2015) so we would struggle to compute the proposal density for a move to a topology more than one SPR move away. In practice, we choose for  $Q$  a mixture of local kernels  $\{Q_m\}_m$ , where each  $Q_m$  proposes a tractable modification of the current state by modifying only one of its components.

The 19 local kernels  $\{Q_m\}_m$  we use are described in detail in Appendix C, and listed in Table 1 therein. Broadly speaking, the following classes of proposals are of interest for this work:

- Subtree prune-and-regraft (SPR) proposals are a primary mechanism for exploring the space of rooted topologies, whereby we randomly select a node and reattach its parent along a randomly chosen branch of the tree. Figure 3 illustrates a simple SPR move.
- We propose to change a single node’s time by sampling on the interval between its eldest child and parent, or we may propose to scale groups of nodes times. Proposals which violate clade or ancestry constraints are rejected so we want to minimise the probability of this occurring.
- Catastrophes interact with moves on the tree topology and branch lengths and must be accounted for in our calculations. We make proposals on the catastrophe set by addition or deletion of a single catastrophe, changing a catastrophe’s position within a branch or moving it to a neighbouring branch, and resampling the entire catastrophe set on a branch with a draw from the prior.

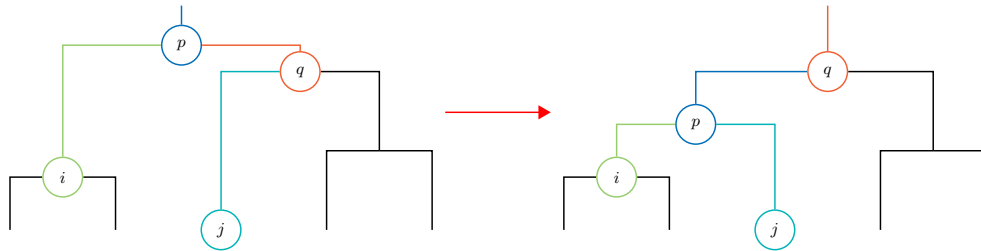


Figure 3: Example of a subtree prune-and-regraft proposal. The edge leading into node  $i$  is detached and its parent  $p$  is reattached along the branch from  $j$  to its parent  $q$  which then becomes the root in the candidate state. For the reverse move, we detach  $p$  and reattach it on the branch into  $q$ .

- Scalar parameters are updated by standard random-walk kernels.

Constructing an MCMC algorithm which efficiently explores the space of phylogenetic trees is an ongoing problem. As SPR-type operators are the primary mechanism for exploring the space of topologies, the corresponding SPR distance introduces a natural metric on the space of topologies. Whidden and Matsen IV (2015) construct a graph where topologies, represented as vertices, are connected if there is an SPR move that transforms one into the other. They find that topologies with high posterior support are frequently isolated from each other by multiple SPR moves; that is, phylogenetic posteriors are naturally multimodal when distance is measured by the number of MCMC steps to transition between states. Whidden and Matsen IV (2017) further analyse properties of the SPR graph. Chains which move more frequently produce lower asymptotic variances (Peskun, 1973) so some form of adaptive MCMC algorithm (Haario et al., 2001) is a component of many standard phylogenetics software packages. Höhna and Drummond (2012) develop Metropolised Gibbs proposal distributions for tree topologies so that a different topology is always proposed at each iteration, while Baele et al. (2017) develop adaptive methods for phylogenetic model parameters; both of these schemes are available in BEAST (Suchard et al., 2018). Douglas et al. (2021) develop adaptive proposal schemes in BEAST 2 (Bouckaert et al., 2019). MrBayes (Ronquist et al., 2012) uses parallel tempering to increase exploration between modes.

Having obtained samples from one or more chains targeting the posterior distribution, we now turn our attention to assessing whether the chains actually mixed well and converged to their stationary distribution.

### 2.3 Diagnosing convergence of phylogenetic MCMC samplers

Although the MCMC algorithm we describe on the space of phylogenetic models is Harris recurrent (Drummond et al., 2002), its finite-sample behaviour is largely unknown as theoretical analyses of Markov chains on the space of phylogenies are restricted to relatively simple settings. Aldous (2000) and Evans and Winter (2006) study random walks on the space of trees through simple rearrangement operations. Mossel and Vigoda



(2006) derive bounds on the Total Variation mixing time for Markov chains on the space of trees and show that MCMC can be misleading when the data arises from a mixture distribution. Practitioners typically resort to the comparison of several runs of the same algorithm from different initial states to check that graphical and numerical summaries stabilise as chains converge; the variation across chains should diminish as their number and length increase (Nascimento et al., 2017). However, as we describe below, the summaries used are often marginal on each parameter or use low-dimensional projections from the space of trees, so their power to detect convergence is unknown.

**Tracer** (Rambaut et al., 2018) takes parameter samples from single or multiple chains and produces visual and numerical summaries for comparison. Graphical summaries include marginal and joint traceplots, histograms and contour plots for the parameter samples and corresponding prior, likelihood and posterior values at each iteration. Tracer also reports summary statistics such as an estimated Effective Sample Size (ESS) for each parameter. The **TopologyTracer** tool within **BEAST** (Suchard et al., 2018) computes the distance between a reference tree and each tree visited by the MCMC; available distance metrics include those proposed by Robinson and Foulds (1981) and Kendall and Colijn (2016). The output can then be loaded into Tracer for further analysis. Recommendations for a minimum target ESS for each parameter vary; under the assumption of normality, Guimarães Fabreti and Höhna (2021) suggest 625. **MrBayes** (Ronquist et al., 2012) uses the Potential Scale Reduction Factor (Gelman and Rubin, 1992) as a convergence diagnostic for tree branch lengths and parameters. Kim et al. (2020) define an  $L_2$ -medoid with respect to their distance metrics then assess convergence of their MCMC samplers by plotting the distance between a running  $L_2$ -medoid and one computed with all of the samples.

In an unrooted tree, which we can form by deleting the root node in a rooted phylogeny and, each edge corresponds to a bipartite split of the taxa. The tree in Figure 2 supports the following non-trivial splits:  $\{2, 3 | \dots\}$ ,  $\{4, 5 | \dots\}$ ,  $\{2, 3, 4, 5 | \dots\}$ ,  $\{6, 7 | \dots\}$  and  $\{6, 7, 8 | \dots\}$ . We can recover a tree topology from a set of compatible splits (Bryant and Moulton, 1999), and splits form the basis of a variety of phylogenetic analysis schemes (Moulton and Bryant, 2004; Allman et al., 2017).

A number of methods attempt to diagnose convergence of MCMC schemes on trees by analysing the projection of sampled topologies onto the space of splits. Beiko et al. (2006) compare the posterior distributions on splits from an extremely long chain to multiple shorter chains and conclude that likelihood traceplots often stabilise well before the corresponding distributions across splits. Are We There Yet? (AWTY) (Nylander et al., 2008) presents trace plots of split frequencies across multiple independent runs as well as cumulative split frequencies, split presence/absence and tree distances within and across chains. Guimarães Fabreti and Höhna (2021) propose a Kolmogorov–Smirnov test on split frequency distributions.

The Average Standard Deviation of Split Frequencies (ASDSF) is widely used as a convergence diagnostic. For a given sampling window, **MrBayes** (Ronquist et al., 2012, 2020) evaluates the ASDSF by first computing the standard deviation of frequencies for each sampled split across the chains and then averages over the splits. By default, **MrBayes** runs two independent quartets of parallel-tempered chains and discards splits



which did not appear in at least 10% of the samples in one of the chains. `MrBayes` can use ASDSF as a stopping rule, in which case its default setting is to stop when the ASDSF falls below 0.01 calculated on the most recent 75% of samples so far. In any case, the ASDSF will depend on the number of chains and window over which it is computed.

The R ([R Core Team, 2021](#)) package `RWTY` ([Warren et al., 2017](#)) provides a suite of tools based on split frequencies; as well those proposed for `AWTY`, `RWTY` also computes cumulative sliding window estimates of ASDSF across chains then plots them with various interval estimates. [Gill et al. \(2020\)](#) use a combination of `RWTY` and `Tracer` to assess convergence in online MCMC-based phylodynamic inference. When a new data set arrives, they add it to the current MCMC state with imputed initial values, then continue the MCMC until the ASDSF decreases below 0.05 before storing samples.

Although the ASDSF will go to 0 as the chains converge, its behaviour has only been studied empirically. [Whidden and Matsen IV \(2015\)](#) find the ASDSF from two independent or parallel-tempered schemes is often insufficient for diagnosing non-convergence in multimodal problems. [Fourment et al. \(2019\)](#) remark that “Typically an ASDSF below 0.01 is taken to be evidence that two MCMC analyses are sampling the same distribution,” but instead use the root mean squared deviation in their study and propose cut-offs for *good agreement*, *acceptable agreement* and *substantial disagreement* with the ground truth. They also compare split distributions using the Kullback–Leibler divergence and obtain broadly similar conclusions.

[Whidden and Matsen IV \(2015\)](#) use the SPR distance to identify bottlenecks in posterior distributions that are difficult to cross for MCMC algorithms using SPR proposals. The authors propose a number of graphical tools for visualising tree space. One of the methods they propose is to construct a graph of topologies visited by an MCMC chain, where each node is a topology weighted by its posterior mass, and edges are weighted by SPR distance or the number of MCMC transitions between them. [Whidden and Matsen IV \(2015\)](#) also propose a topological variation of the Potential Scale Reduction Factor using the SPR distance which empirically exhibits similar behaviour to ASDSF.

[Lanfear et al. \(2016\)](#) propose to assess convergence on topologies by plotting a distance, such as the path or Robinson–Foulds distance, between pairs of sampled trees against the number of transitions between them by the MCMC. [Lanfear et al. \(2016\)](#) also propose an approximate effective sample size calculation for tree topology samples. These techniques are implemented in `RWTY` ([Warren et al., 2017](#)).

[Harrington et al. \(2020\)](#) present a comprehensive empirical study comparing a variety of heuristic convergence diagnostics, such as requiring all ESS estimates for topology and parameter samples above a given threshold or ASDSF below a threshold, on approximately 18,000 phylogenetic analyses. The authors find similar behaviour between many of the diagnostic tools, but also some incongruence between similar diagnostics.

All of the methods we describe above do not jointly consider the entire model state when diagnosing convergence, and the theoretical properties of those which are asymptotically consistent are not well understood on finite samples. In addition, as the behaviour

of a phylogenetic MCMC algorithm is often specific to the model and data set, we cannot expect a method which only looks at part of the sampled state to perform well on a wide variety of problems. In the following section, we describe how to couple Markov chains for phylogenetic problems to estimate the total variation bound in Equation 1 to diagnose convergence on the entire parameter space.

### 3 Coupled MCMC for phylogenetic inference

#### 3.1 Coupling generic MCMC transition kernels

A coupling of two distributions  $p$  and  $q$  on a general space  $\mathcal{X}$  is a joint distribution  $\gamma$  on  $\mathcal{X} \times \mathcal{X}$  whose first marginal is  $p$  and second  $q$ ; that is,  $\gamma(A, \mathcal{X}) = p(A)$  and  $\gamma(\mathcal{X}, A) = q(A)$  for any measurable set  $A \subset \mathcal{X}$ . If we can evaluate  $p$  and  $q$  at every point in  $\mathcal{X}$ , then we can construct  $\gamma$  to be a maximal coupling:  $\mathbb{P}(X = Y)$  is maximised for  $(X, Y) \sim \gamma$ . Maximal couplings are typically not unique; one general construction of a maximal coupling is the following (Jacob et al., 2020):

1. Sample  $X \sim p$  and  $U \sim \text{U}(0, 1)$
2. If  $U \leq q(X)/p(X)$ , then  $Y \leftarrow X$
3. Otherwise, draw  $Y' \sim q$  and  $U' \sim \text{U}(0, 1)$  until  $U' > p(Y')/q(Y')$ , then  $Y \leftarrow Y'$ .

We can check that the marginal distributions are correct and that  $\mathbb{P}(X = Y) = \int (p \wedge q)(dx)$  for  $(X, Y)$  drawn in this manner. The expected cost of this algorithm is constant but its variance increases as  $d_{\text{TV}}(p, q)$  decreases (Jacob et al., 2020). We discuss algorithms to sample from maximal couplings in more detail in Algorithm B.

We now consider two chains Markov chains  $(X_t)$  and  $(Y_t)$  on  $\mathcal{X}$  with common invariant distribution  $\pi$ , Markov transition kernel  $P$  and Metropolis–Hastings proposal distribution  $Q$ . From initial states  $X_0$  and  $Y_0$ , Jacob et al. (2020) draw  $X_1 \sim P(X_0, \cdot)$  from the marginal kernel, and at each subsequent iteration  $t > 1$  draw  $(X_t, Y_{t-1}) \sim \bar{P}((X_{t-1}, Y_{t-2}), \cdot)$ , a coupling of  $P(X_{t-1}, \cdot)$  and  $P(Y_{t-2}, \cdot)$ . Jacob et al. (2020) construct  $\bar{P}$  by separately sampling proposals and acceptance indicators from maximal couplings of their respective distributions.

1. Sample proposals  $(X', Y')$  from  $\bar{Q}((X_{t-1}, Y_{t-2}), \cdot)$ , a maximal coupling of  $Q(X_{t-1}, \cdot)$  and  $Q(Y_{t-2}, \cdot)$
2. Sample acceptance indicators  $(B_X, B_Y)$  from a maximal coupling of  $\text{Bern}(\alpha(X_{t-1}, X'))$  and  $\text{Bern}(\alpha(Y_{t-2}, Y'))$ 
  - $U \sim \text{U}(0, 1)$
  - If  $U \leq \alpha(X_{t-1}, X')$  then  $B_X = 1$ , otherwise  $B_X = 0$
  - If  $U \leq \alpha(Y_{t-2}, Y')$  then  $B_Y = 1$ , otherwise  $B_Y = 0$
3. Set  $X_t = B_X X' + (1 - B_X) X_{t-1}$  and  $Y_{t-1} = B_Y Y' + (1 - B_Y) Y_{t-2}$ .

Although this is not a maximal coupling of the transition kernels, [Jacob et al. \(2020\)](#) demonstrate that this widely applicable approach produces meeting times which satisfy the validity assumptions for their algorithm. [Wang et al. \(2021\)](#) describe techniques to sample directly from  $\bar{P}$ . To debias Monte Carlo estimators based on samples  $k, \dots, m$ , [Jacob et al. \(2020\)](#) run their lag-1 algorithm for  $m \vee \tau$  iterations. In order to estimate bounds such as in Equation 1, [Biswas et al. \(2019\)](#) initialise the  $X$  chain with  $l > 1$  iterations of  $P$  and run their algorithm until coupling. We refer the reader to [Jacob et al. \(2020\)](#) and [Biswas et al. \(2019\)](#) for further details on this strategy and how to build unbiased estimators from the output, and note that the strategy can remain valid even if the couplings are not maximal.

We follow [Jacob et al. \(2020\)](#) and [Biswas et al. \(2019\)](#) and separately sample proposals and acceptance indicators from couplings of their respective distributions. We cannot sample from a maximal coupling of many of the proposal distributions for moves on the phylogeny as we cannot evaluate the proposal densities for complete moves. However, by breaking these proposals into a sequence of steps and sampling from a maximal coupling at each, we produce a non-trivial coupling of the transition kernels and a distribution on coupling times which decays at most geometrically. One point to note is that the chains must have the same transition kernel at each iteration, otherwise two chains which meet could later separate, so we do not consider adaptive schemes here. However, we could obtain a distribution on proposals from a pilot adaptive run on a given problem and use that in the coupled algorithm.

### 3.2 Tree and model notation

Before we can describe our method to implement the ideas of Section 3.1 to MCMC on a space of phylogenetic trees, we give some notation. We assume that the set of observed taxa  $L$  are the terminal outcome at the leaves of a stochastic process along a rooted phylogenetic tree  $g$ , where each observed taxon corresponds to a leaf of the tree. We abuse notation and also use  $L$  to refer to the number of taxa. A rooted tree with  $L$  leaves has  $L - 1$  internal nodes representing the most recent common ancestors of their descendent leaves, of which the *root* is the most recent common ancestor of all the leaves. Let  $E$  and  $V$  denote the edge and vertex sets of the tree. Each node  $i \in V$  has an associated time  $t_i$  and  $T$  is the set of node times. Let  $C$  index the set of catastrophes on the tree, where each catastrophe has an associated branch and a location along it. We define  $g = (E, V, T, C)$  as our dated phylogeny with catastrophes. The remaining parameters of the SD model are continuous parameters in  $\mathbb{R}_+$  or  $(0, 1)$ .

### 3.3 Housekeeping

Many of the proposals which affect the tree or catastrophes involve first sampling a target node or branch  $i$  followed by a sequence of proposals which depend on  $i$ . Only the leaf nodes in states  $X$  and  $Y$  are labelled, the internal node indices are arbitrary, so in order to sample from maximal couplings of moves on the tree we need to identify corresponding components in  $X$  and  $Y$ . Inspired by [Steel and Warnow \(1993\)](#), we do *housekeeping* on the states in advance of every move so that nodes with common descendent leaves have identical indices in both trees. Figure 4 illustrates this operation. Thus, when a node or subtree exists in both  $X$  and  $Y$ , we maximally couple all moves

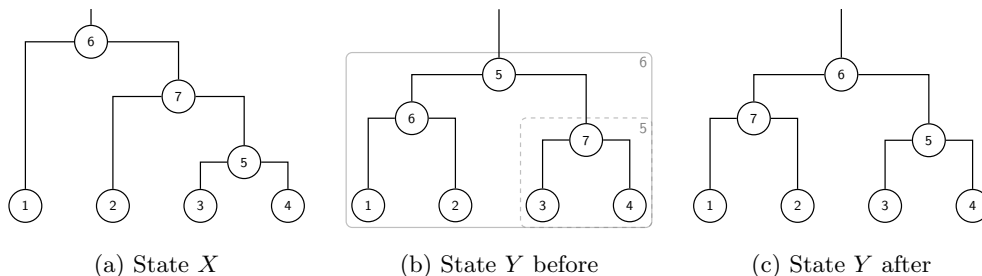


Figure 4: Housekeeping state  $Y$  to match  $X$  where possible. We assign the same indices to internal nodes with common descendent leaves. The subtree with leaves 3 and 4 is common to both states so we assign its root the same index, likewise the root of the entire tree. The labelling of the remaining internal nodes is arbitrary.

related to it. For example, if we have selected the move type which updates a single node time, we (a) apply that move type to both  $X$  and  $Y$ ; (b) if the node selected for  $X$  exists in  $Y$ , the probability that we select the same node for  $Y$  is maximised; (c) we maximally couple the proposal distributions. The move has the same effect in both states if we target the same components, and in any case preserves the marginal properties of the move. This way, each component of the state has an opportunity to couple, and the two chains come gradually closer. As states  $X$  and  $Y$  become closer together, the probability of a move having the same effect in both states increases.

Housekeeping is key to the success of our algorithm. Without this housekeeping operation, we essentially sample from an independent coupling of distributions on nodes or branches so it is unlikely to satisfy the requirement on the distribution of  $\tau$  (Jacob et al., 2020), indeed we found this to be the case in practice. Algorithm 1 describes our implementation of the coupled MCMC algorithm of Biswas et al. (2019) with housekeeping after each iteration.

### 3.4 Coupling proposal distributions

At each step of our coupled Metropolis–Hastings algorithm, we first maximally couple the selection of the proposal distribution. As the weights on each proposal are constant throughout the algorithm, this amounts to randomly selecting a move and using it in both chains. As in Jacob et al. (2020) and Biswas et al. (2019), we maximally couple the accept-reject step separately from the proposal.

Each member of our family of proposal distributions acts primarily on a component of either the topology  $(E, V)$ , the node times  $T$ , the catastrophe set  $C$ , or one of the scalar parameters of the SD model. A move on the topology may also affect the node times, catastrophes or rate parameters, and a move on node times affects the location of catastrophes. Sampling from a coupling of proposals for the parameters of the SD model is trivial as they are either positive rate parameters or constrained to  $(0, 1)$ , but in order for the distributions to overlap we require the other elements of the states to be close.

---

**Algorithm 1** Lag- $l$  coupled MCMC algorithm of Biswas et al. (2019) with housekeeping operation.

---

**Input:** Initial states  $X_0$  and  $Y_0$ , lag  $l$

**for**  $t = 1$  to  $l$  **do**

$X_t \sim P(X_{t-1}, \cdot)$  ▷ Marginal MCMC kernel

$X' \sim Q(X_{t-1}, \cdot)$

$B_X \sim \text{Bern}(\alpha(X_{t-1}, X'))$

$X_t \leftarrow B_X X' + (1 - B_X) X_{t-1}$

**end for**

$Y_0 \leftarrow \text{HOUSEKEEPING}(X_t, Y_0)$

**while**  $X_t \neq Y_{t-l}$  **do**

$t \leftarrow t + 1$

$(X_t, Y_{t-l}) \sim \bar{P}((X_{t-1}, Y_{t-l-1}), \cdot)$  ▷ Coupling of marginal kernels

$(X', Y') \sim \bar{Q}((X_{t-1}, Y_{t-l-1}), \cdot)$

$U \sim \text{U}(0, 1)$

$X_t \leftarrow X'$  if  $U \leq \alpha(X_{t-1}, X')$ , otherwise  $X_t \leftarrow X_{t-1}$

$Y_{t-l} \leftarrow Y'$  if  $U \leq \alpha(Y_{t-l-1}, Y')$ , otherwise  $Y_{t-l} \leftarrow Y_{t-l-1}$

$Y_{t-l} \leftarrow \text{HOUSEKEEPING}(X_t, Y_{t-l})$

**end while**

$\tau \leftarrow t$

**Output:**  $\tau$ ,  $\{X_0, X_1, \dots, X_\tau\}$  and  $\{Y_0, Y_1, \dots, Y_{\tau-l}\}$

---

We now describe how to couple some of these proposals and provide a full description in Appendix C. For the remainder of this section, let  $X$  and  $Y$  denote the current state of the lag- $l$  staggered chains and  $X'$  and  $Y'$  proposals drawn from  $\bar{Q}((X, Y), \cdot)$ .

### Structural moves

Recall the subtree prune-and-regraft move in Figure 3 where we select a node  $i$ , detach its parent  $p$  and reattach it elsewhere on the tree. In its simplest form, we can propose an SPR move from  $X$  to  $X'$  via the following sequence of steps:

1. Select a node  $i$  uniformly from the nodes below the root, let  $p$  denote its parent
2. Select a destination branch  $\langle q, j \rangle$  uniformly from the branches on the tree, node  $q$  is  $j$ 's parent
3. Sample a new time  $t'_p$  uniformly along the destination branch.

We form the proposed state then by detaching  $p$  and reattaching it to the tree along branch  $\langle q, j \rangle$  at time  $t'_p$ . The move fails if the destination is invalid, for example because the destination is on the subtree or the move violates clade or time constraints, so in practice our proposal reduces the probability of that occurring. If catastrophes are included in the model, then we also propose to update their number and locations on branches affected by the SPR move.

To couple this proposal, we sample from a maximal coupling at each step of the move. In combination with housekeeping, we make SPR proposals that bring the states closer together and we reduce the probability of making proposals which would decouple components of the topology. Sampling from a maximal coupling of the entire SPR proposals would be computationally expensive; as the acceptance rate of SPR proposals is often quite low, we do not expect that a maximal coupling of the overall move would significantly change the distribution on coupling times. Appendix C.2 describes our couplings of topology proposals in detail.

### **Node times and model parameters**

When proposing to update a single node time, we select the same node in both states; through housekeeping, this will correspond to the same component of the tree if it exists. We then sample the new node times from a maximal coupling of the corresponding distributions, and given that resample the catastrophes on affected branches from a maximal coupling of their distributions. Our marginal kernel also includes proposals to scale groups of ancestral node times by a common factor  $\nu \sim U(1/2, 2)$ . This cannot in general produce a coupling of the corresponding node times in the two states. In practice, we attempt to couple the tree or subtree root node times and scale the remaining nodes accordingly. In our experiments, we observed that disabling this move reduced the coupling time but include them in our kernel to aid exploring the posterior; Heng and Jacob (2019) discuss the trade-off between coupling and optimal parameter configurations for Hamiltonian Monte Carlo sampling. We describe these proposals and how to couple them in detail in Appendix C.3

### **Catastrophes**

For each catastrophe on the tree, we store its branch index and relative time along the branch. Our proposals for changing the number of catastrophes on the tree are motivated by our Poisson process prior on their distribution. We propose to add catastrophes uniformly at random on tree and delete or move catastrophes selected at random from those already on it (Geyer and Møller, 1994) through Reversible Jump MCMC proposals (Green, 1995). Maximal couplings of these moves are not well defined when the trees do not match, so as above we break them into sub-steps and sample from a maximal coupling at each.

The probability of removing the same catastrophe, identified by its branch and relative location along it, from states  $X$  and  $Y$  then depends on the intersection of the catastrophe locations on the target branch across the two states. When proposing to resample the catastrophes set on a branch, we simulate a dominating point process from the prior and maximally couple the inclusion of individual catastrophes in the two states.

In addition to a rate  $\rho$ , catastrophes have a common strength parameter  $\kappa$ . Strong catastrophes are more identifiable but can induce local modes in the posterior. Weak catastrophes are comparatively easy to modify as they have less effect on the likelihood, but they are also less identifiable in the model. By coupling MCMC chains, we can identify these failures to mix through pairs of chains which fail to meet and develop moves to facilitate better mixing. We discuss these issues with coupling over catastrophes

further in Section 4.2 and describe our catastrophe proposals and couplings in detail in Appendix C.4.

### 3.5 Software

We implemented our algorithm in TraitLab (Nicholls et al., 2013), a Matlab (The MathWorks, Inc., 2021) toolbox for fitting SD models, and the code is publicly available on GitHub.<sup>1</sup> We have also made available our scripts to generate synthetic data sets, run experiments and analyse the output.<sup>2</sup>

Jacob et al. (2020) discuss the computational cost of inference when sampling from couplings. In our experiments, the computational cost of updating a pair of chains with a sample from our coupled kernel was just over twice that for a single draw from the marginal kernel. There was additional computational overhead due to the housekeeping operation and testing for equality between trees. Note however that using couplings allows us to fully use the increasingly available power of parallel computing.

## 4 Experiments

We illustrate our coupled MCMC approach on synthetic and real data sets. In building a Bayesian model, we can analytically integrate a number of parameters out our posterior, namely the trait birth rate  $\lambda$  and catastrophe rate  $\rho$ . Additionally, in the absence of lateral transfer we can integrate out the locations of catastrophes within branches. The SD model is only weakly identifiable without additional constraints on branch lengths, rate parameters and the catastrophe process; we discuss these issues in the context of each experiment.

For each of our experiments, and for various lags, we run 100 pairs of chains targeting the posterior distribution. Each pair of chains is initialised by independent short MCMC runs targeting the prior without catastrophes. We then run our coupled approach until the chains meet; as we only store every 100th iteration, there is a loss of resolution in our estimate of the coupling time  $\tau$ . Using the coupling times for each lag, we estimate the total variation bound on convergence in Equation 1. As a by-product of the output, we can also keep only one chain from each pair and obtain 100 independent chains targeting the posterior: this allows us to compute the convergence statistics of Section 2 as a comparison. We compute our estimated TV bound from 100 pairs of chains, and the ASDSF from 100 marginal chains (the  $X$  component of the coupled chains for the highest lag) on 10 disjoint sampling windows, which we obtained by modifying RWTY (Warren et al., 2017); we followed the default choice in MrBayes and only considered splits which appeared in at least 10% of the samples for one or more chains. All of the figures were created using ggplot2 (Wickham, 2016) in R (R Core Team, 2021).

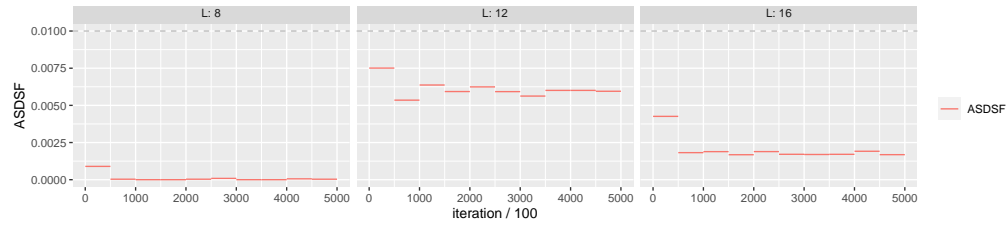
### 4.1 Basic SD model

We illustrate our approach on a simple version of the SD model without missing data or catastrophes. We first randomly generated trees with 8, 12 and 16 leaves, and rescaled

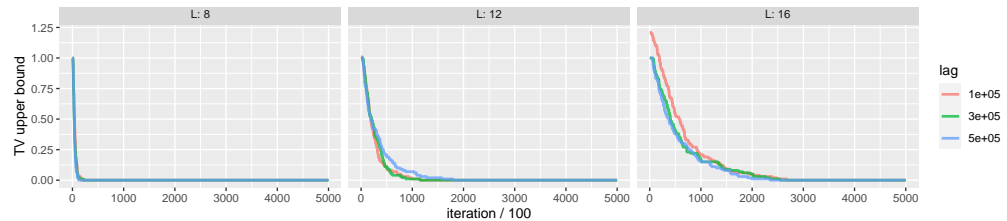
<sup>1</sup><https://github.com/lukejelly/TraitLab>

<sup>2</sup><https://github.com/lukejelly/CoupledPhylogenetics>

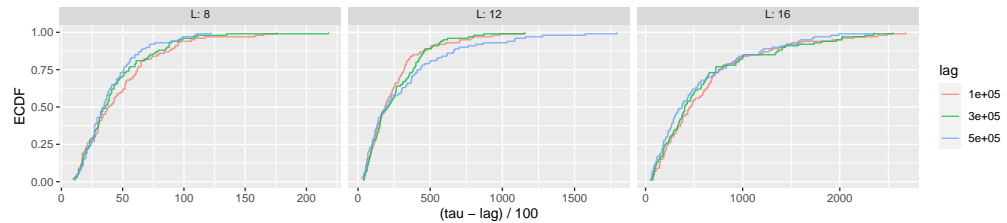




(a) Average standard deviation of split frequencies on disjoint sliding windows of 500 samples ( $5 \times 10^4$  MCMC iterations) across 100 chains.



(b) Estimated TV bounds from 100 pairs of coupled chains across a range of lags.



(c) ECDFs of coupling times showing geometric tail behaviour.

Figure 5: Comparison of average standard deviation of split frequencies against estimated total variation bounds on synthetic data sets with  $L = 8, 12$  and  $16$  taxa. In contrast to ASDSF, our estimated TV bounds clearly indicate convergence.

the branch lengths so that the root time was  $10^3$  in each. We then simulated data from the SD model with birth rate  $\lambda = 0.1$  and death rate  $\mu = 2.5 \times 10^{-4}$  using the Gillespie algorithm (Gillespie, 1977). The target of our inference was the posterior distribution on tree topologies and branch lengths as we fixed  $\mu$  at the value used to generate the data and integrated  $\lambda$  out analytically with respect to its prior. We set  $2 \times 10^3$  as the upper bound on the root time and did not impose any clade constraints. Figure 5 displays the results of our experiments.

In Figure 5a, we see that the ASDSF is well below 0.01 for each of the data sets, although that threshold is based on a different sliding window in MrBayes (Ronquist et al., 2020). We see some variation in ASDSF estimates for  $L = 12$  and  $16$  leaves before they stabilise; in any case, it is difficult to say what level of variation is reasonable for diagnosing convergence. Using only two or ten chains for each figure produced noisier

estimates on similar ranges.

Our estimated TV bounds in Figure 5b diagnose convergence on the entire sample space so we have more confidence in our estimates. The bounds reach 0 within a few thousand iterations for  $L = 8$  leaves but require up to  $3 \times 10^5$  iterations when  $L = 16$ . The estimates are stable across lags and we do not see plateaus which would be caused by slow mixing across modes in the target distribution (Biswas et al., 2019). The empirical cumulative distribution function (ECDF) of the coupling times in Figure 5c displays the desired geometric tail behaviour.

## 4.2 SD model with catastrophes

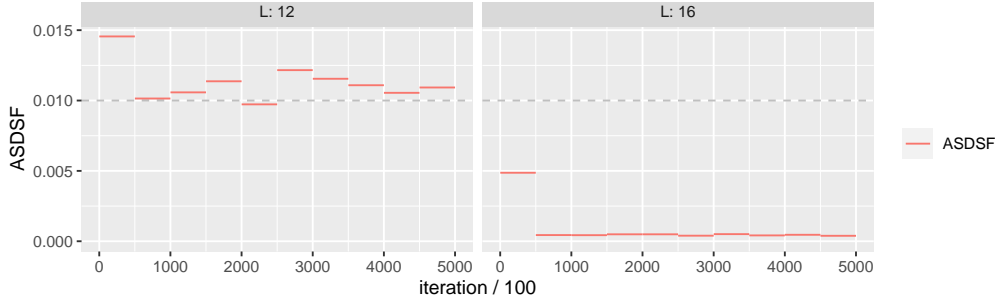
We now consider situations where the model is not identifiable, and demonstrate how attempting to couple the MCMC can help diagnose this modelling issue. Mixing over catastrophes is an issue for the model as each catastrophe introduces a discrete change in the likelihood. The effective duration of a catastrophe is  $-\log(1 - \kappa)/\mu$  units of time, so multiple combinations of  $\mu$  and  $\kappa$  can produce the same effective duration. In addition, multiple weak catastrophes on a branch can mimic a stronger one. We consider the problems posed by both weak and strong catastrophes so generated data and fit the SD model with the following settings

- Three catastrophes with strength  $\kappa = 1/20$  and a  $\Gamma(1.5, 5000)$  prior on  $\rho$
- Two catastrophes with strength  $\kappa = 1/3$  and a  $\Gamma(1.5, 10^5)$  prior on  $\rho$ .

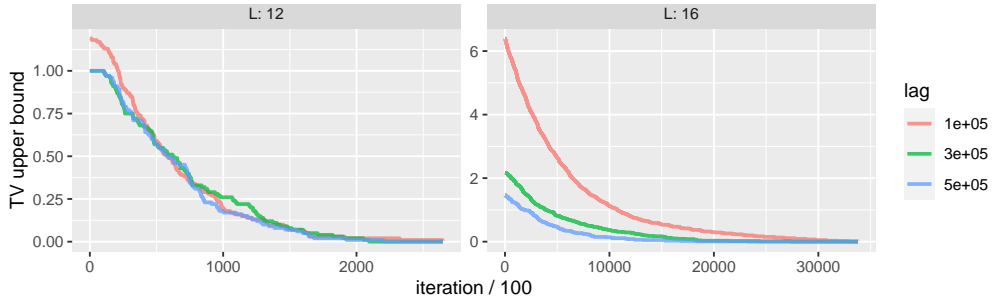
We used the 12- and 16-leaf trees from Section 4.1 then placed catastrophes on randomly selected branches leading into leaf nodes before generating the data. We sampled a clade at random for each tree and data set before fitting the model. The true presence/absence state of a trait at leaf  $i \in L$  was observed with probability  $\xi_i \sim \text{Beta}(1, 1/3)$ , and marked missing otherwise. For these experiments, we fixed  $\mu$  and  $\kappa$  at the values used to generate the data and attempt to infer topology and node times, the number of catastrophes on each branch and the missing data parameters.

Figure 6 displays the results of our experiments with weak catastrophes. For the data with  $L = 12$  leaves, the ASDSF estimates vary around 0.01 while our estimated TV bounds are stable across lags and reach 0 within  $2.5 \times 10^5$  iterations. Our estimated TV bounds indicate a clear failure to mix when  $L = 16$ , with some pairs of chains requiring up to  $3 \times 10^6$  iterations to couple. In contrast, the ASDSF remains stable and close to 0, suggesting convergence when it has not occurred.

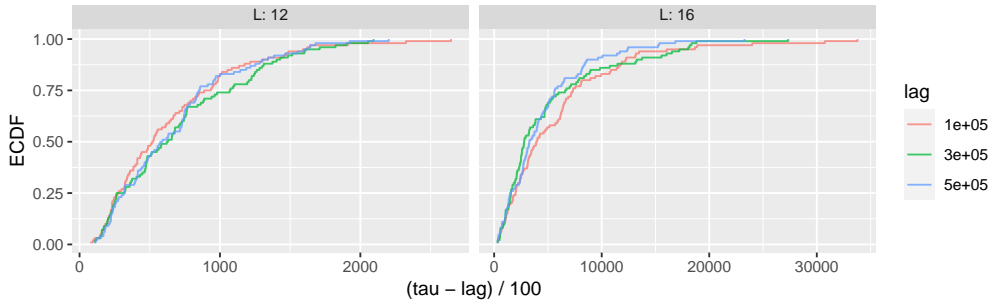
We display the results of our experiments with strong catastrophes and a more stringent prior on their number in Figure 7. The variation in ASDSF estimates is low beyond the first window of  $5 \times 10^4$  MCMC iterations. For  $L = 12$ , some pairs of chains at lag of  $5 \times 10^5$  coupled much later than the rest, with the corresponding TV bound reaching 0 much later than for lower lags. For  $L = 16$ , we see some variation in TV bounds across lags, particularly for the lowest lag. In both cases, further analysis at higher lags is required in order to safely diagnose convergence.



(a) ASDSF on disjoint sliding windows of 500 samples ( $5 \times 10^4$  MCMC iterations) across 100 chains.

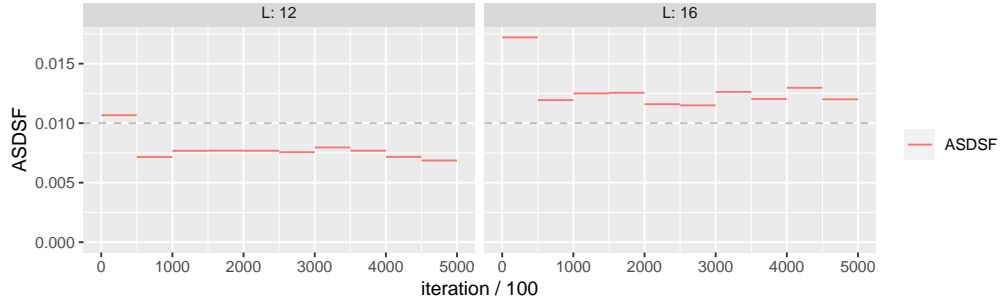


(b) Estimated TV bounds from 100 pairs of coupled chains at each lag.

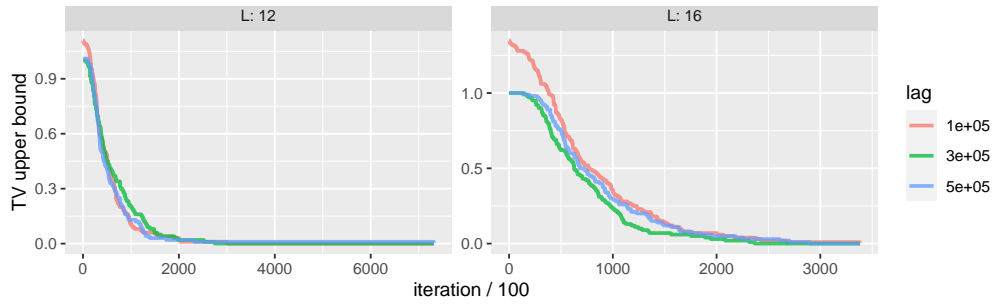


(c) ECDFs of coupling times.

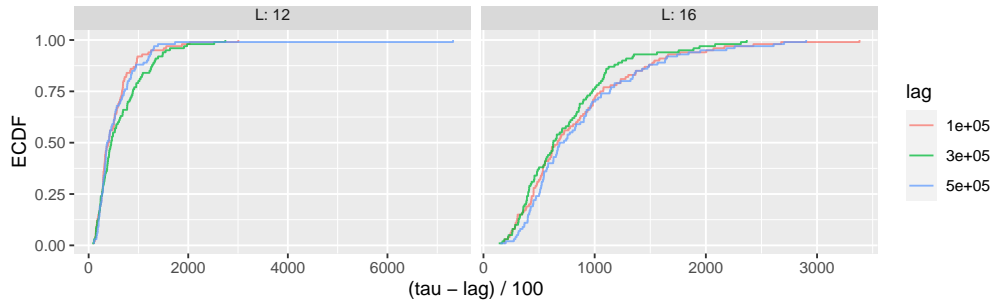
Figure 6: ASDSF and estimated TV bounds on synthetic data sets with  $L = 12$  and  $16$  taxa, three weak catastrophes and a weak prior on the number of catastrophes. The TV bounds indicate that our MCMC algorithm struggled to mix on the 16-leaf data set, with some pairs of chains taking over  $3 \times 10^6$  iterations to couple; ASDSF fails to diagnose this behaviour.



(a) ASDSF on disjoint sliding windows of 500 samples (each covering  $5 \times 10^4$  MCMC iterations) across 100 chains.



(b) Estimated TV bounds from 100 pairs of coupled chains at each lag.



(c) ECDFs of coupling times.

Figure 7: ASDSF and estimated TV bounds on synthetic data sets with  $L = 12$  and  $16$  taxa, two strong catastrophes and more restrictive prior on the number of catastrophes. The coupling times for some of the 12-leaf experiments were significantly higher than the rest so the corresponding estimated TV bounds were slow to reach 0.

### 4.3 Lexical trait data in Eastern Polynesian languages

We revisit the analysis by [Kelly and Nicholls \(2017\)](#) of lexical trait data in Eastern Polynesian languages under the SD model with lateral trait transfer. The data is drawn from the Austronesian Basic Vocabulary Database ([Greenhill et al., 2017](#)) and is a subset of languages analysed by [Gray et al. \(2009\)](#) analysed under a number of model-based Bayesian approaches, including Stochastic Dollo, and [Gray et al. \(2010\)](#) using *Neighbor-Net*, a likelihood-free method for constructing phylogenetic networks from splits. [Gray et al. \(2009\)](#) found evidence of lateral trait transfer between languages and [Kelly and Nicholls \(2017\)](#) reached similar conclusions comparing the SD model with and without lateral trait transfer.

We fit the SD model with lateral transfer at rate  $\beta$  so must also infer the location of catastrophes along branches. For these experiments, we fixed  $\kappa = 1/3$  and allowed both  $\mu$  and  $\beta$  to vary. Following [Gray et al. \(2009\)](#), [Kelly and Nicholls \(2017\)](#) imposed a single clade constraint to fix the root age of the tree to [1150, 1800] years before the present and we do the same here.

The lateral trait transfer model is extremely computationally expensive as the likelihood computation grows exponentially in the number of taxa, so is an ideal candidate for coupling as we do not want to waste resources on inefficient burn-in estimates and would like to make use of experiments run in parallel. For the 11 taxa in this data set,  $10^6$  iterations of the marginal MCMC algorithm takes approximately 12 hours.

Figure 8 displays the results of our experiments. The ASDSF estimates vary closely around 0.04 for each window. Our estimated TV bounds are consistent across lags and reach 0 within  $4 \times 10^5$  iterations. From trace plots, histograms and effective sample sizes in marginal chains, [Kelly and Nicholls \(2017\)](#) estimated that  $10^6$  MCMC iterations were required to reach convergence when fitting the lateral transfer model to this data set. Our coupling approach thus produces a significantly lower estimate of the convergence time and we have much more confidence in our results.

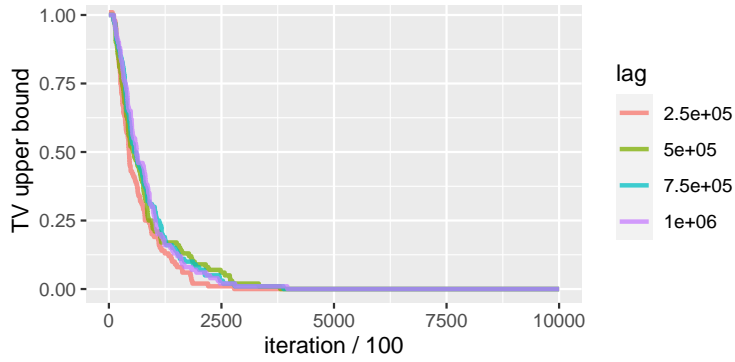
## 5 Concluding remarks

Couplings provide a theoretical and practical framework for assessing the convergence of MCMC samplers. It shows benefits both for practitioners using MCMC on phylogenies for applied problems, and for statisticians constructing new models or proposition kernels.

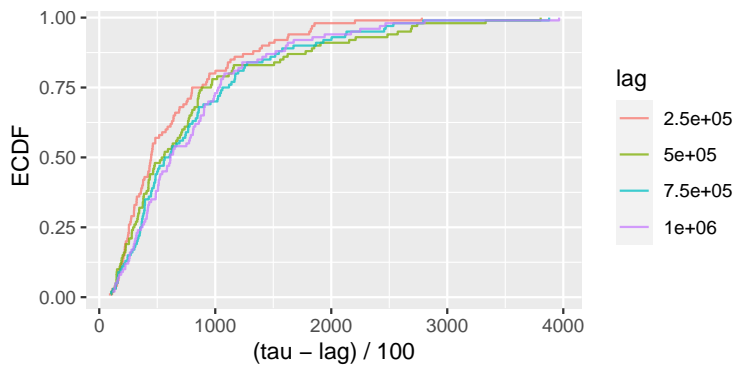
For practitioners, the coupling approach provides a practical bound on the TV distance, rather than existing ad hoc approaches. It gives a global guarantee of convergence, instead of focusing on certain marginal distributions. In addition to providing a more trustworthy check of convergence, we notice in some of our experiments that convergence is detected earlier than with other methods: once the chains have reached stationarity, the coupling method is faster to detect it than other approaches, potentially giving better estimates of the number of iterations to remove as burn-in and of the mixing time. We remind the reader that the chains should not be interrupted as soon as they have coupled, but should be then allowed to run for many further iterations so that they give an acceptable sample from the posterior. This is even more important because of



(a) Average standard deviation of split frequencies on disjoint sliding windows of 1000 MCMC samples (thinned from  $10^9$  MCMC iterations) in 100 chains.



(b) TV bounds on tree and model parameters from 100 pairs of coupled chains.



(c) ECDF of coupling times displaying geometric tail behaviour.

Figure 8: Estimating convergence of the SD with lateral transfer model fit to Eastern Polynesian lexical trait data.

the following remark: the coupling event is highly unlikely to occur before the chains have reached stationarity, and it is thus reasonable to assume that the burn-in is shorter than the coupling time; on the other hand, the state of the chain at the coupling time  $X_\tau$  cannot be assumed to follow the posterior, as coupling may be easier for certain values in the region of high posterior density. Overall, since MCMC on phylogenies is typically run for a very large number of iterations and is very time consuming, we hope that coupled MCMC will allow practitioners to use the MCMC output more efficiently.

The coupling approach is also of use earlier in the pipeline, as a tool to help identify certain modelling issues and weaknesses in the MCMC kernel. In our experiments with small catastrophes (low value of  $\kappa$ ), some parameters are poorly identified and this leads to high multimodality in the posterior, which the MCMC sampler has trouble exploring. Our initial attempts to couple the chains failed in this situation, which made the issue fully apparent and allowed us to improve the marginal kernels. In other experiments, we have sometimes observed  $X$  and  $Y$  to be in very similar states but to have difficulty coupling, and have found this to be due to needing to update simultaneously two highly correlated components of the state. If the mixture of kernels does not allow for a proposal which updates the two components jointly, such transitions hardly ever occur and the mixing time deteriorates. Diagnosing why the chains are not coupling makes this issue more obvious, and helps us construct a more efficient kernel, or detect some problems associated with multimodality or ancillarity. These ideas are left for future works.

Previous discussions of coupling MCMC, such as those described in [Jacob et al. \(2020\)](#), have focused on using couplings to construct unbiased estimators. This is also possible in the phylogeny case, but we have found it less useful as it is hardly applicable to topology estimation. We however underline the fact that unbiased estimators can be obtained as a byproduct of the algorithm. In this paper, we have focused on coupling the Metropolis–Hastings algorithm. In situations where other MCMC methods prove more efficient at exploring the posterior, such as sequential Monte Carlo ([Wang et al., 2019](#)) or Hamiltonian Monte Carlo ([Bastide et al., forthcoming](#)), it could be useful to adapt these coupling methods following ideas in [Heng and Jacob \(2019\)](#) or [Jacob et al. \(2019\)](#).

## References

- D.J. Aldous. Mixing time for a Markov chain on cladograms. *Combin. Probab. Comput.*, 9(3):191–204, 2000.
- A.V. Alekseyenko, C.J. Lee, and M.A. Suchard. Wagner and Dollo: a stochastic duet by composing two parsimonious solos. *Syst. Biol.*, 57(5):772–784, 2008.
- E.S. Allman, L.S. Kubatko, and J.A. Rhodes. Split Scores: A Tool to Quantify Phylogenetic Signal in Genome-Scale Data. *Syst. Biol.*, 66(4):620–636, 1 2017.
- G. Baele, P. Lemey, A. Rambaut, and M.A. Suchard. Adaptive MCMC in Bayesian phylogenetics: an application to analyzing partitioned data in BEAST. *Bioinformatics*, 33(12):1798–1805, 02 2017.



- L.S.T. Bastide, P. and Ho, G. Baele, P. Lemey, and M.A. Suchard. Efficient Bayesian Inference of General Gaussian Models on Large Phylogenetic Trees. *Ann. Appl. Stat.*, forthcoming.
- R.G. Beiko, J.M. Keith, T.J. Harlow, and M.A. Ragan. Searching for Convergence in Phylogenetic Markov Chain Monte Carlo. *Syst. Biol.*, 55(4):553–565, 08 2006.
- L.J. Billera, S.P. Holmes, and K. Vogtmann. Geometry of the space of phylogenetic trees. *Adv. Appl. Math.*, 27(4):733–767, 2001.
- N. Biswas, P.E. Jacob, and P. Vanetti. Estimating convergence of Markov chains with  $L$ -lag couplings. In *NeurIPS*, pages 7389–7399, 2019.
- N. Biswas, A. Bhattacharya, P.E. Jacob, and J.E. Johndrow. Coupled Markov chain Monte Carlo for high-dimensional regression with Half-t priors. *arXiv:2012.04798*, 2020.
- N. Bou-Rabee and A. Eberle. Couplings for Andersen Dynamics. *arXiv:2009.14239*, 2020.
- A. Bouchard-Côté, Kevin C., D. Cubranic, S. Hosseini, J. Hume, M. Lepur, Z. Ouyang, and G. Sgarbi. Blang: Bayesian declarative modelling of general data structures and inference via algorithms based on distribution continua. *arXiv:1912.10396*, 2021.
- R. Bouckaert, T.G. Vaughan, J. Barido-Sottani, S. Duchêne, M. Fourment, A. Gavryushkina, J. Heled, G. Jones, D. Kühnert, N. De Maio, M. Matschiner, F.K. Mendes, N.F. Müller, H.A. Ogilvie, L. du Plessis, A. Poppinga, A. Rambaut, D. Rasmussen, I. Siveroni, M.A. Suchard, C. H. Wu, D. Xie, C. Zhang, T. Stadler, and A.J. Drummond. BEAST 2.5: An advanced software platform for Bayesian evolutionary analysis. *PLOS Comput. Biol.*, 15(4), 04 2019.
- D. Bryant and V. Moulton. A polynomial time algorithm for constructing the refined Buneman tree. *Appl. Math. Lett.*, 12(2):51–56, 1999.
- J. Douglas, R. Zhang, and R. Bouckaert. Adaptive dating and fast proposals: Revisiting the phylogenetic relaxed clock model. *PLOS Comput. Biol.*, 17(2):1–30, 02 2021.
- A.J. Drummond, G.K. Nicholls, A.G. Rodrigo, and W. Solomon. Estimating mutation parameters, population history and genealogy simultaneously from temporally spaced sequence data. *Genetics*, 161(3):1307–1320, 2002.
- S.N. Evans and A. Winter. Subtree prune and regraft: A reversible real tree-valued Markov process. *Ann. Probab.*, 34(3):918 – 961, 2006.
- J. Felsenstein. Evolutionary trees from DNA sequences: a maximum likelihood approach. *J. Mol. Evol.*, 17(6):368–376, 1981.
- M. Fourment, A.F. Magee, C. Whidden, A. Bilge, F.A Matsen IV, and V.N. Minin. 19 Dubious Ways to Compute the Marginal Likelihood of a Phylogenetic Tree Topology. *Syst. Biol.*, 69(2):209–220, 08 2019.
- A. Gelman and D.B. Rubin. Inference from iterative simulation using multiple sequences. *Stat. Sci.*, 7(4):457–472, 1992.

- C.J. Geyer and J. Møller. Simulation procedures and likelihood inference for spatial point processes. *Scand. J. Stat.*, pages 359–373, 1994.
- M.S. Gill, P. Lemey, M.A. Suchard, A. Rambaut, and G. Baele. Online Bayesian Phylogenetic Inference in BEAST with Application to Epidemic Reconstruction. *Mol. Biol. Evol.*, 37(6):1832–1842, 02 2020.
- D.T. Gillespie. Exact stochastic simulation of coupled chemical reactions. *J. Phys. Chem.*, 81(25):2340–2361, 1977.
- R.D. Gray, A.J. Drummond, and S.J. Greenhill. Language phylogenies reveal expansion pulses and pauses in Pacific settlement. *Science*, 323(5913):479–483, 2009.
- R.D. Gray, D. Bryant, and S.J. Greenhill. On the shape and fabric of human history. *Philos. T. R. Soc. B*, 365(1559):3923–3933, 2010.
- P.J. Green. Reversible jump Markov chain Monte Carlo computation and Bayesian model determination. *Biometrika*, 82(4):711–732, 1995.
- S.J. Greenhill, C.-H. Wu, X. Hua, M. Dunn, S.C. Levinson, and R.D. Gray. Evolutionary dynamics of language systems. *Proc. Natl. Acad. Sci. USA*, 114(42):E8822–E8829, 2017. ISSN 0027-8424.
- L. Guimarães Fabreti and S. Höhna. Convergence Assessment for Bayesian Phylogenetic Analysis using MCMC simulation. *bioRxiv*, 2021.
- H. Haario, E. Saksman, and J. Tamminen. An adaptive Metropolis algorithm. *Bernoulli*, 7(2):223 – 242, 2001.
- S.M. Harrington, V. Wishingrad, and R.C. Thomson. Properties of Markov Chain Monte Carlo Performance across Many Empirical Alignments. *Mol. Biol. Evol.*, 11 2020.
- W.K. Hastings. Monte Carlo sampling methods using Markov chains and their applications. *Biometrika*, 57(1):97–109, 1970.
- J Heng and P.E. Jacob. Unbiased Hamiltonian Monte Carlo with couplings. *Biometrika*, 106(2):287–302, 02 2019.
- S. Höhna and A.J. Drummond. Guided Tree Topology Proposals for Bayesian Phylogenetic Inference. *Syst. Biol.*, 61(1):1–11, 08 2012.
- S. Höhna, M.J. Landis, T.A. Heath, B. Boussau, N. Lartillot, B.R. Moore, J.P. Huelsenbeck, and F. Ronquist. RevBayes: Bayesian Phylogenetic Inference Using Graphical Models and an Interactive Model-Specification Language. *Syst. Biol.*, 65(4):726–736, 05 2016.
- P.E. Jacob, F. Lindsten, and T.B. Schön. Smoothing with couplings of conditional particle filters. *J. Am. Stat. Assoc.*, 2019.
- P.E. Jacob, J. O’Leary, and Y.F. Atchadé. Unbiased Markov chain Monte Carlo methods with couplings. *J. Roy. Statist. Soc. B*, 2020.

- L.J. Kelly and G.K. Nicholls. Lateral transfer in Stochastic Dollo models. *Ann. Appl. Stat.*, 11(2):1146–1168, 2017.
- M. Kendall and C. Colijn. Mapping Phylogenetic Trees to Reveal Distinct Patterns of Evolution. *Mol. Biol. Evol.*, 33(10):2735–2743, 06 2016.
- J. Kim, N.A. Rosenberg, and J.A. Palacios. Distance metrics for ranked evolutionary trees. *Proc. Natl. Acad. Sci. USA*, 117(46):28876–28886, 2020.
- J.F.C. Kingman. *Poisson Processes*. Clarendon Press, Oxford, 1992.
- J. Koskela. Zig-zag sampling for discrete structures and non-reversible phylogenetic MCMC. *arXiv 2004.08807*, 2020.
- R. Lanfear, X. Hua, and D.L. Warren. Estimating the effective sample size of tree topologies from Bayesian phylogenetic analyses. *Genome Biol. Evol.*, 8(8):2319–2332, 2016.
- P. Lemey, N. Ruktanonchai, S.L. Hong, V. Colizza, C. Poletto, F. Van den Broeck, M.S. Gill, X. Ji, A. Levasseur, B.B. Oude Munnink, M. Koopmans, A. Sadilek, S. Lai, A.J. Tatem, G. Baele, M.A. Suchard, and S. Dellicour. Untangling introductions and persistence in COVID-19 resurgence in Europe. *Nature*, pages 1–8, 2021.
- A. McPherson, A. Roth, E. Laks, T. Masud, A. Bashashati, A.W. Zhang, G. Ha, J. Biele, D. Yap, A. Wan, L.M. Prentice, J. Khattra, M.A. Smith, C.B. Nielsen, S.C. Mullaly, S. Kalloger, A. Karnezis, K. Shumansky, C. Siu, J. Rosner, H.L. Chan, J. Ho, N. Melnyk, J. Senz, W. Yang, R. Moore, A.J. Mungall, M.A. Marra, A. Bouchard-Côté, C.B. Gilks, D.G. Huntsman, J.N. McAlpine, S. Aparicio, and S.P. Shah. Divergent modes of clonal spread and intraperitoneal mixing in high-grade serous ovarian cancer. *Nature Genet.*, 48(7):758–767, 2016.
- L. Middleton, G. Deligiannidis, A. Doucet, and P.E. Jacob. Unbiased Markov chain Monte Carlo for intractable target distributions. *Electron. J. Stat.*, 14(2):2842 – 2891, 2020.
- B. Morel, P. Barbera, L. Czech, B. Bettisworth, L. Hübner, S. Lutteropp, D. Serdari, E.-G. Kostaki, I. Mamais, A.M. Kozlov, P. Pavlidis, D. Paraskevis, and A. Stamatakis. Phylogenetic Analysis of SARS-CoV-2 Data Is Difficult. *Mol. Biol. Evol.*, 38(5): 1777–1791, 12 2020.
- E. Mossel and E. Vigoda. Limitations of Markov chain Monte Carlo algorithms for Bayesian inference of phylogeny. *Ann. Appl. Probab.*, 16(4):2215 – 2234, 2006.
- V. Moulton and D. Bryant. NeighbourNet: An agglomerative method for the reconstruction of phylogenetic network. *Mol. Biol. Evol.*, 2(21):255–6, 2004.
- N.F. Müller and R.R. Bouckaert. Adaptive Metropolis-coupled MCMC for BEAST 2. *PeerJ*, 8:e9473, 2020.
- F.F. Nascimento, M. Dos Reis, and Z. Yang. A biologist’s guide to Bayesian phylogenetic analysis. *Nat. Ecol. Evol.*, 1(10):1446–1454, 2017.
- G.K. Nicholls and R.D. Gray. Dated ancestral trees from binary trait data and their

- application to the diversification of languages. *J. Roy. Stat. Soc. B*, 70(3):545–566, 2008.
- G.K. Nicholls and R.J. Ryder. Phylogenetic models for Semitic vocabulary. In D. Conesa, A. Forte, A. López-Quílez, and F. Muñoz, editors, *Proceedings of the International Workshop on Statistical Modelling*, pages 431–436, 2011.
- G.K. Nicholls, R.J. Ryder, and D. Welch. *TraitLab: a MatLab Package for Fitting and Simulating Binary Trait-Like Data*, 2013.
- J.A.A. Nylander, J.C. Wilgenbusch, D.L. Warren, and D.L. Swofford. AWTY (are we there yet?): a system for graphical exploration of MCMC convergence in Bayesian phylogenetics. *Bioinformatics*, 24(4):581–583, 2008.
- P.H. Peskun. Optimum Monte-Carlo sampling using Markov chains. *Biometrika*, 60(3): 607–612, 1973.
- R Core Team. *R: A Language and Environment for Statistical Computing*. R Foundation for Statistical Computing, Vienna, Austria, 2021. URL <https://www.R-project.org/>.
- A. Rambaut, A.J. Drummond, D. Xie, G. Baele, and M.A. Suchard. Posterior Summarization in Bayesian Phylogenetics Using Tracer 1.7. *Syst. Biol.*, 67(5):901–904, 04 2018.
- D.F. Robinson and L.R. Foulds. Comparison of phylogenetic trees. *Math. Biosci.*, 53 (1–2):131–147, 1981. ISSN 0025-5564.
- F. Ronquist, M. Teslenko, P. Van Der Mark, D.L. Ayres, A. Darling, S. Höhna, B. Larget, L. Liu, M.A. Suchard, and J.P. Huelsenbeck. MrBayes 3.2: efficient Bayesian phylogenetic inference and model choice across a large model space. *Syst. Biol.*, 61(3):539–542, 2012.
- F. Ronquist, J.P. Huelsenbeck, M. Teslenko, C. Zhang, and J.A.A. Nylander. Mr-bayes version 3.2 manual: Tutorials and model summaries. [https://github.com/NBISweden/MrBayes/blob/develop/doc/manual/Manual\\_MrBayes\\_v3.2.pdf](https://github.com/NBISweden/MrBayes/blob/develop/doc/manual/Manual_MrBayes_v3.2.pdf), 2020. Accessed 09 August 2021.
- R.J. Ryder and G.K. Nicholls. Missing data in a stochastic Dollo model for binary trait data, and its application to the dating of Proto-Indo-European. *J. Roy. Statist. Soc. C*, 60(1):71–92, 2011.
- L. Sagart, G. Jacques, Y. Lai, R.J. Ryder, V. Thouzeau, S.J. Greenhill, and J.-M. List. Dated language phylogenies shed light on the ancestry of Sino-Tibetan. *Proc. Natl. Acad. Sci. USA*, 116(21):10317–10322, 2019.
- Y.S. Song. On the combinatorics of rooted binary phylogenetic trees. *Ann. Comb.*, 7 (3):365–379, 2003.
- M. Steel and T. Warnow. Kaikoura tree theorems: Computing the maximum agreement subtree. *Inf. Process. Lett.*, 48(2):77–82, 1993.
- M.A. Suchard, P. Lemey, G. Baele, D.L. Ayres, A.J. Drummond, and A. Rambaut.

- Bayesian phylogenetic and phylodynamic data integration using BEAST 1.10. *Virus Evol.*, 4(1), 06 2018.
- The MathWorks, Inc. *Matlab Release 2021a*. Natick, Massachusetts, United States, 2021.
- G. Wang, J. O’Leary, and P. Jacob. Maximal Couplings of the Metropolis-Hastings Algorithm . In A. Banerjee and K. Fukumizu, editors, *Proceedings of The 24th International Conference on Artificial Intelligence and Statistics*, volume 130 of *Proceedings of Machine Learning Research*, pages 1225–1233. PMLR, 13–15 Apr 2021.
- L. Wang, S. Wang, and A. Bouchard-Côté. An Annealed Sequential Monte Carlo Method for Bayesian Phylogenetics. *Syst. Biol.*, 69(1):155–183, 06 2019.
- D.L. Warren, A.J. Geneva, and R. Lanfear. RWTY (R We There Yet): An R Package for Examining Convergence of Bayesian Phylogenetic Analyses. *Mol. Biol. Evol.*, 34(4):1016–1020, 01 2017. R package version 1.0.2.
- J. Watts, O. Sheehan, Q.D. Atkinson, J. Bulbulia, and R.D. Gray. Ritual human sacrifice promoted and sustained the evolution of stratified societies. *Nature*, 532(7598):228–231, 2016.
- C. Whidden and F.A. Matsen IV. Quantifying MCMC Exploration of Phylogenetic Tree Space. *Syst. Biol.*, 64(3):472–491, 01 2015.
- C. Whidden and F.A. Matsen IV. Ricci–Ollivier curvature of the rooted phylogenetic subtree–prune–regraft graph. *Theor. Comput. Sci.*, 699:1–20, 2017.
- C. Whidden, B.C. Claywell, T. Fisher, A.F. Magee, M. Fourment, and F.A. Matsen IV. Systematic Exploration of the High Likelihood Set of Phylogenetic Tree Topologies. *Syst. Biol.*, 69(2):280–293, 08 2019.
- H. Wickham. *ggplot2: Elegant Graphics for Data Analysis*. Springer-Verlag New York, 2016. ISBN 978-3-319-24277-4.
- A. Willis. Confidence sets for phylogenetic trees. *J. Am. Stat. Assoc.*, 114(525):235–244, 2019.
- A. Willis and R. Bell. Uncertainty in phylogenetic tree estimates. *J. Comput. Graph. Stat.*, 27(3):542–552, 2018.
- C. Zhang and F.A. Matsen IV. Variational Bayesian Phylogenetic Inference. In *ICLR*, 2019.
- Z. Zhang, A. Nishimura, P. Bastide, X. Ji, R.P. Payne, P. Goulder, P. Lemey, and M.A. Suchard. Large-scale inference of correlation among mixed-type biological traits with phylogenetic multivariate probit models. *Ann. Appl. Stat.*, 15(1):230 – 251, 2021.

### Acknowledgments

We are grateful to Pierre E. Jacob for helpful discussions during this project. LJK is supported by the French government under management of Agence Nationale de la Recherche as part of the ABSint programme, reference ANR-18-CE40-0034.

## Appendix A: Stochastic Dollo model

Figure 2 illustrates a trait history drawn from the Stochastic Dollo model on a phylogeny. The SD model posits a birth-death process of traits along the tree: new traits arise in each species according to a Poisson process with rate  $\lambda$  and instances of each trait die independently at rate  $\mu$ . We record the binary patterns of trait presence or absence across the leaves. For an ordering of the leaf nodes, let  $N_p$  denote the number of traits displaying binary pattern  $p \in \mathcal{P} \subseteq \{0, 1\}^L$ . A branch of infinite length leads into the root node so the process is in equilibrium with a  $\text{Poisson}(\lambda/\mu)$  number of traits just before the first branching event. With this initial condition, the tree and model parameters, we can compute the expected frequency  $z_p(\lambda) = \mathbb{E}[N_p | g, \lambda, \mu]$  of each binary pattern by integrating over the possible unobserved trait events on the tree (Nicholls and Gray, 2008). As we have a Poisson process of trait births with independent thinning, our observation model is

$$N_p \sim \text{Poisson}(z_p), \quad p \in \mathcal{P}. \quad (2)$$

The expected frequencies grow linearly with  $\lambda$ ; that is,  $z_p(\lambda) = \lambda z_p(1)$ , so we now write  $z_p$  for  $z_p(1)$ . In building our Bayesian model, we place a  $\Gamma(a, b)$  prior on  $\lambda$  and analytically integrate it out of our model to obtain a Negative Multinomial distribution on the pattern frequencies,

$$(N_p)_p \sim \text{NM} \left( a, \frac{b}{b + \sum_q z_q}, \left( \frac{z_p}{b + \sum_q z_q} \right)_p \right). \quad (3)$$

We incorporate a number of extensions to the basic observation model.

**Rate heterogeneity through catastrophes** We allow for discrete bursts of evolutionary activity in the form of a *catastrophes* which arise according to a Poisson process of rate  $\rho$  along the branches of the tree. At a catastrophe, each trait present on the branch is killed with probability  $\kappa$  and a  $\text{Poisson}(\lambda\kappa/\mu)$  number of new traits are born. This is equivalent to instantaneously advancing the trait process by  $-\log(1 - \kappa)/\mu$  units of time on the branch. The branch leading into the root is infinitely long so we do not consider catastrophes on it. Catastrophes are reversible with respect to the underlying trait process so we cannot identify the location of a catastrophe along a branch and only consider the number of catastrophes on each branch.

**Missing-at-random data** We assume that data is missing at random, so the true status of a trait at leaf  $i \in L$  is observed with probability  $\xi_i$  and recorded as missing otherwise (Ryder and Nicholls, 2011).

**Lateral trait transfer** Lateral trait transfer is a form of reticulate evolutionary activity whereby species can acquire traits outside of ancestral relationships. Following Kelly and Nicholls (2017), each instance of a trait transfers a copy of itself to other contemporary species at rate  $\beta$ . As in the birth-death SD model, a catastrophe advances the trait process along the branch by  $-\log(1 - \kappa)/\mu$  units of time including trait transfers in from other branches. A catastrophe is not reversible in this setting as its effect depends

on the number of other branches and the number of traits on them, so we model the location of catastrophes along their branches.

Figure 2 illustrates each of these processes. These extensions do not change the Poisson nature of the data in Equation 2 or Negative Multinomial in Equation 3, but do require a more complicated integral to compute the expected pattern frequencies (Ryder and Nicholls, 2011; Kelly and Nicholls, 2017).

We place diffuse priors on all of the parameters. Our tree prior is Uniform across topologies and approximately Uniform on the time of the root node (Nicholls and Ryder, 2011). Clade constraints restrict the space of possible topologies and node times and are incorporated into the prior distribution. We can integrate the catastrophe rate  $\rho$  out of our posterior with respect to a Gamma prior to obtain a Negative Multinomial distribution of catastrophe counts on branches. Conditional on their number, the prior distribution of catastrophe locations on a branch is Uniform. Multiple small catastrophes on a branch can produce a similar effect to a single larger catastrophe, so we generally opt to fix  $\kappa$  at a reasonable value rather than infer it. Under the full model, the target of our inference is  $X = (g, \mu, \beta, \Xi)$ , where the tree  $g = (E, V, T, C)$  includes the topology  $(E, V)$ , node times  $T$  and catastrophes  $C$ , and  $\Xi = (\xi_i)_{i \in L}$  gathers the missing data parameters.

## Appendix B: Sampling from maximal couplings

For random variables  $X \sim p$  and  $Y \sim q$  on a common space, we consider two approaches to sampling  $(X, Y)$  from a maximal coupling of  $p$  and  $q$ .

We use the following approach, previously described in Section 3.1, for the majority of our couplings (Jacob et al., 2020, Algorithm 2).

1. Sample  $X \sim p$  and  $U \sim U(0, 1)$
2. If  $U \leq q(X)/p(X)$  then set  $Y \leftarrow X$
3. Otherwise draw  $Y' \sim q$  and  $U' \sim U(0, 1)$  until  $U' > p(Y')/q(Y')$  then return  $Y \leftarrow Y'$

For suitable  $p$  and  $q$ , we use the following approach to sampling from a maximal coupling (Jacob et al., 2020, Section 5.4).

1. With probability  $[p \wedge q] = \int (p \wedge q)(dx)$ ,

$$X \leftarrow Y \sim \frac{p \wedge q}{[p \wedge q]}$$

2. Otherwise

$$X \sim \frac{p - p \wedge q}{1 - [p \wedge q]} \quad \text{and} \quad Y \sim \frac{q - p \wedge q}{1 - [p \wedge q]}.$$

This approach was tractable for rescaling parameters by Uniform random variables and sampling new root times in SPR moves, as the following example describes.



**Two Shifted Exponential distributions**

We denote  $\text{Exp}(\theta; c)$  an  $\text{Exp}(\theta)$  random variable restricted to be greater than  $c$ , and  $\text{Exp}(\theta; c, d)$  when restricted to  $[c, d)$ .

We would like to sample  $X \sim p = \text{Exp}(\theta; a_p)$  and  $Y \sim q = \text{Exp}(\theta; a_q)$ . With probability  $[p \wedge q] = \exp(-\theta|a_p - a_q|)$ , we sample from the overlap between the distributions, so

$$X \leftarrow Y \sim \text{Exp}(\theta; a_p \vee a_q).$$

Otherwise, we sample independently. If  $a_p < a_q$ , then we draw

$$\begin{aligned} X &\sim \text{Exp}(\theta; a_p, a_q) = a_p - \theta^{-1} \log[1 - U_x(1 - e^{-\theta(a_q - a_p)})], \\ Y &\sim \text{Exp}(\theta; a_q) = a_q - \theta^{-1} \log(U_y), \end{aligned}$$

where  $U_x$  and  $U_y \sim U(0, 1)$ . If  $a_q < a_p$  then we change the sampling distributions accordingly.

**Appendix C: Coupling proposals for phylogenetic models**

Our proposal distribution  $Q$  is a mixture of various local moves  $(Q_m)_m$ ; Table 1 lists the various proposals in our MCMC algorithm. As the weights on each move are constant, we can sample from a maximal coupling by proposing the same proposal operator to both chains; that is, at each iteration  $t \geq l$  we sample a single  $Q$  from the available moves  $(Q_m)_m$  and use it to draw proposals in both the  $X$  and  $Y$  chains. We now give a detailed description of each marginal move and how we couple sampling from it. Our proposal distributions are not optimal in terms of mixing or convergence — for example, we may make invalid proposals which are automatically rejected — but are tractable and sufficient to be useful in practice.

**C.1 Notation**

A phylogenetic tree  $g = (E, V, T, C)$  has edge set  $E$ , vertex set  $V$ , node times  $T$  and catastrophes  $C$ . The neighbours of a node  $i \in V$  are its parent  $\text{pa}(i)$ , offspring  $\text{off}(i) = \{j : \text{pa}(j) = i\}$  and sibling  $\text{sib}(i) = \{j \neq i : \text{pa}(j) = \text{pa}(i)\}$ . In Figure 1,  $\text{pa}(3) = 1$ ,  $\text{sib}(3) = 2$  and  $\text{off}(3) = \emptyset$ . Let  $T$  denote the set of node times  $\{t_i : i \in V\}$ . We refer to the edge  $\langle \text{pa}(i), i \rangle$  into node  $i$  as branch  $i$  and denote its length  $\Delta_i = t_{\text{pa}(i)} - t_i$ ; let  $\Delta$  denote the length of the tree beneath the root. We abuse notation and use  $L$  to both denote the set of indices of leaf nodes as well as the number of leaves. We denote  $r$  the root of the tree and  $A = V \setminus L$  the set of  $L - 1$  ancestral nodes; although there is an infinitely long branch leading into the root, we ignore its parent node when referring to  $A$  or  $V$ .

Leaf node indices are identical and constant across states  $X$  and  $Y$ . Through our house-keeping operation, the root node indices are identical across states  $X$  and  $Y$  at each iteration, but are not constant across iterations. As a node cannot move outside its clade, the set of indices within a given clade is also identical across  $X$  and  $Y$ , so each clade subtree will have a common root at each iteration after housekeeping.

Table 1: MCMC moves act on the tree topology, node times, catastrophes, and parameters of the trait diversification or observation process.

Primary target	Section	Move	Description
Topology	C.2	1	Exchange parents of neighbouring node pair
		2	Exchange parents of randomly chosen node pair
		3	SPR onto neighbouring branch
		4	SPR onto randomly chosen branch
Times	C.3	5	Resample internal node time
		6	Resample leaf time
		7	Rescale tree
		8	Rescale subtree
		9	Rescale tree above clade bounds
Catastrophes	C.4	10	Add catastrophe to an edge
		11	Delete catastrophe from an edge
		12	Move catastrophe to neighbouring edge
		13	Resample all catastrophes on branch
		14	Resample catastrophe location on branch
SD parameters	C.5	15	Rescale $\mu$
		16	Rescale $\beta$
		17	Rescale $\kappa$
		18	Rescale one element of $\Xi$
		19	Rescale all elements of $\Xi$

## C.2 Moves 1–4: tree topology

### Moves 1 & 2: subtree swap

In a subtree swap move, we switch the parents of a pair of nodes  $i$  and  $j$ ; that is,

$$\begin{aligned} \text{pa}(i)' &\leftarrow \text{pa}(j), \\ \text{pa}(j)' &\leftarrow \text{pa}(i). \end{aligned}$$

For a *narrow* move (1 in Table 1), we select  $i$  and  $j$  as follows:

1. Sample node  $i \sim U(i' : \text{pa}(i') \neq r)$
2. Set  $j \leftarrow \text{sib}[\text{pa}(i)]$
3. if  $t_j \geq t_{\text{pa}(i)}$  or any clade constraints are violated then the move fails

For a *wide* move (2), we draw  $(i, j)$  uniformly from the valid pairs; that is, those which are not neighbours or violate any clade or ancestry constraints.

In both the narrow and wide cases, we can easily draw from a maximal coupling of the corresponding discrete Uniform distributions.

**Moves 3 & 4: subtree prune-and-regraft**

As illustrated in Figure 3 and Section 3.4, we randomly choose a subtree with root  $i$ , detach its parent  $\text{pa}(i)$  from the tree and reattach it at new time  $t'_p$  on branch  $j$ . In the proposed state,

$$\begin{aligned}\text{pa}[\text{pa}(i)]' &\leftarrow \text{pa}(j), \\ \text{pa}[\text{sib}(i)]' &\leftarrow \text{pa}(j), \\ \text{pa}(j)' &\leftarrow \text{pa}(i).\end{aligned}$$

To simplify notation, for the rest of this section we denote  $p = \text{pa}(i)$  and  $q = \text{pa}(j)$ .

In a narrow SPR move (3), we

1. Sample node  $i \sim U(V)$
2. Set  $j \leftarrow \text{sib}(p)$
3. Sample a new time  $t'_p \sim U(t_i \vee t_j, t_q)$ .

The move fails if  $p = r$ .

For a wide SPR move (4), we sample  $i$  as above and destination  $j$  uniformly from branches in the same clade, or the entire tree including the root branch if we do not impose clades. The move fails if  $t_q \leq t_i$ , as we cannot propose a valid time for  $p$ , or if the edges  $\langle p, i \rangle$  and  $\langle q, j \rangle$  have a node in common. If  $j$  is currently an internal branch, then  $t'_p$  is sampled as above, but if  $j = r$ , then  $t'_p \sim \text{Exp}(\theta; t_j)$ .

We sample from maximal couplings at each step of these moves. If the proposal fails for one state at an intermediate step, then we proceed as in the marginal move for the remainder of the move in the other state.

If catastrophes are included in the model then we also update them in an SPR move. Let  $n_v$  denote the number of catastrophes currently on branch  $v = \langle \text{pa}(v), v \rangle$ . As the length of branch  $i$  changes in the proposal, we rescale the times of catastrophes on  $i$  accordingly. This introduces a Jacobian term in the ratio of proposal densities in the Metropolis–Hastings acceptance probability  $\alpha$ , although it is cancelled out by the ratio of prior distributions. As the branch leading into the root is infinitely long, we do not consider catastrophes on it. We move any catastrophes currently on branch  $p$  onto  $h = \text{sib}(i)$  in the new state, and  $p$  acquires a Binomial sample of the catastrophes currently on the destination branch  $j$ ; that is,

$$\begin{aligned}n'_h &\leftarrow n_h + n_p, \\ n'_j &\leftarrow \text{Binomial}\left(n_j, \frac{t'_p - t_j}{t_q - t_j}\right), \\ n'_p &\leftarrow n_j + n'_j.\end{aligned}$$

If instead  $p$  becomes the root, then it loses its catastrophes and  $n'_j$  is sampled from the prior in the new state, likewise  $n'_h$  if  $h$  becomes the root in the new state.

We sample  $n'_j$  in the proposed states for each chain from a maximal coupling of their respective distributions; given  $n'_j$ , the catastrophe updates on the remaining branches are deterministic. This is different to what was previously implemented by [Ryder and Nicholls \(2011\)](#) and [Kelly and Nicholls \(2017\)](#) for the marginal move. This is a situation where we were able to diagnose an issue with the marginal kernel thanks to the coupling.

We also refresh the locations of catastrophes on branches  $j$ ,  $h$  and  $p$ . We sample from a maximal coupling of the distributions of locations along branches given their respective counts; we describe this procedure in detail in [Section C.4](#).

### C.3 Moves 5–9: resampling or rescaling node times

These moves change the length of one or more node times. When rescaling multiple node times by a common factor, we cannot sample from a maximal coupling so instead sample from a maximal coupling for one of the nodes and rescale the rest accordingly, we describe this in detail in the relevant sections. The times of any catastrophes are rescaled accordingly, any Jacobian terms in the Metropolis–Hastings ratio are cancelled by the ratio of priors on catastrophes in the two states.

#### Move 5: resample internal node time

For this move, we sample an internal node  $i$  at random and propose to change its time.

- Sample  $i \sim U(A)$ ; let  $t_j = \max_{j' \in \text{off}(i)} t_{j'}$
- If  $i = r$ , then  $t_i \sim U(\frac{t_i+t_j}{2}, 2t_i - t_j)$ ; otherwise  $t_i \sim U(t_j, t_{\text{pa}(i)})$ .

When coupling, we always sample the same  $i$  in both states, and if it is the root in one state then it will also be the root in the other. We then sample from a maximal coupling of the new node time distributions.

We also resample catastrophe counts and locations on the branches connected to  $i$ . Let  $j$  and  $k$  denote the offspring of  $i$ . If  $i$  is not the root, then we sample new catastrophe counts as

$$(n'_i, n'_j, n'_k) \sim \text{Multinomial} \left( n_i + n_j + n_k, \left( \frac{\Delta'_i}{\Delta'_{ijk}}, \frac{\Delta'_j}{\Delta'_{ijk}}, \frac{\Delta'_k}{\Delta'_{ijk}} \right) \right),$$

where  $\Delta'_i$  is length of branch  $i$  in the proposed state, and  $\Delta'_{ijk} = \Delta'_i + \Delta'_j + \Delta'_k$ . If  $i$  is the root, then we only resample catastrophe counts on  $j$  and  $k$ . We sample from a coupling of Multinomial distributions if the total catastrophe count on  $i$ ,  $j$  and  $k$  is equal in both states, otherwise we sample independently. We describe how to couple sampling the locations in [Section C.4](#).

#### Move 6: resample leaf time

For certain taxa, we may only know the range on which it was sampled rather than the exact time. For this move, we select a leaf at random and propose a new time sampled uniformly at random along its range. If the new leaf time is greater than its parent then

the move fails. When sampling from a coupling here, we choose the same node in both states, and as the proposed time is independent of the current state, we always sample the same node time in both.

#### **Move 7: rescale tree**

For this move, we rescale the tree by  $\eta \sim U(1/2, 2)$ . Let  $t_0$  denote the age of the youngest leaf node, typically 0, then

$$t'_i \leftarrow t_0 + \nu(t_i - t_0), \quad i \in A. \quad (4)$$

If the death rate  $\mu$  is being sampled then we set  $\mu' \leftarrow \mu/\nu$  so that the expected number of trait deaths remains constant; we apply the same update to  $\beta$  when accounting for lateral transfer. The move fails if any leaf node is older than its parent in the proposed state.

We cannot sample from a maximal coupling of all the new node times, so instead we sample from a maximal coupling of the root time distributions and scale the other internal nodes accordingly; that is, we sample

$$t'_r \sim U\left(t_0 + \frac{t_r - t_0}{2}, 2t_r - t_0\right), \quad (5)$$

and use  $\nu = (t'_r - t_0)/(t_r - t_0)$  for the update in Equation 4.

#### **Move 8: rescale sub tree**

We sample a subtree root  $i$  with probability proportional to its size, the number of leaves beneath it, then rescale it by  $\nu \sim U(1/2, 2)$ . For this move, the update is identical to Equation 4 except we only consider the subtree nodes and  $t_0$  is the youngest leaf of the subtree. This move fails if the new subtree root age is older than its parent or any leaf node is older than its parent.

As in the move to rescale the entire tree, we cannot sample from a maximal coupling of all the subtree node times. Instead, we sample the subtree root  $i$  in each state from a maximal coupling of the corresponding distributions in a similar fashion to Equation 5, then update the remaining subtree node times accordingly.

#### **Move 9: rescale tree above clade bounds**

Similar to moves 7 and 8, we rescale the tree above clade bounds by  $\nu \sim U(1/2, 2)$ . As in moves 7 and 8, we cannot sample from a maximal coupling from the joint distribution on proposed node times. Instead, we proceed in an identical fashion to move 7 so sample new root times from a maximal coupling of their respective distributions, as described in Equation 5, then rescale the times of nodes above clade bounds according to Equation 4.

### **C.4 Moves 10–14: catastrophes**

Catastrophes are latent variables which we cannot integrate analytically out of our posterior, as described in Appendix A, we only consider catastrophes on branches beneath the root. For the lateral transfer model, each catastrophe  $c = (i, u) \in C$  records its

branch  $i$  and its relative location  $u$  along it; that is, the time of a catastrophe  $c$  is  $t_i + u(t_{\text{pa}(i)} - t_i)$ . Let  $n_i$  denote the number of catastrophes on a branch  $i$  below the root and  $n$  the total on the tree. In the absence of lateral transfer,  $C$  only records the number of catastrophes on each branch.

### Move 10: add one catastrophe

We propose to add a catastrophe uniformly at random across the tree,

1. Select a branch  $b$  with probability  $\Delta_b/\Delta$
2. Sample a relative location  $u \sim \text{U}(0, 1)$
3. Form the proposed state  $C' \leftarrow C \cup \{(b, u)\}$ .

When coupling this move, we first sample the target branch in each state from a maximal coupling of the distributions. As the relative locations are Uniform, we propose the same to both states.

This move is the inverse of move 11 so we give them the same weight in our distribution on proposal kernels.

### Move 11: delete one catastrophe

We select a catastrophe for deletion uniformly at random from those on the tree.

1. Select a branch  $i$  with probability  $n_i/n$
2. Select a catastrophe  $c$  uniformly at random from the  $n_i$  catastrophes on  $i$
3. Form the proposed state  $C' \leftarrow C \setminus \{c\}$ .

If there are no catastrophes on the tree then this move fails.

We first sample the target branch in each state from a maximal coupling. The catastrophes on the target branch are identified by their relative locations, the intersection of these sets may be non-empty if we choose the same branch in both states. We sample from a coupling of discrete Uniform distributions on catastrophe locations, then propose to delete the corresponding catastrophe in each state.

### Move 12: move one catastrophe to a neighbouring edge

We sample a catastrophe at random from those on the tree to move to a neighbouring branch.

1. Select a branch  $i$  with probability  $n_i/n$
2. Select a catastrophe  $c = (i, u)$  uniformly at random from the  $n_i$  catastrophes on  $i$
3. Select a destination  $j \sim \text{U}(\{\text{pa}(i), \text{off}(i), \text{sib}[\text{pa}(i)]\} \setminus \{r\})$ , we ignore the root

4. Sample a new relative location  $u' \sim U(0, 1)$  on the destination branch
5. Form the proposed state  $C' \leftarrow C \cup \{(j, u')\} \setminus \{(i, u)\}$ .

As in move 11, this move fails if there are no catastrophes on the tree.

When coupling this move, we sample the branch  $i$  and catastrophe  $c$  identically to move 11. We then sample the destination branch from a maximal coupling of the discrete Uniform distributions on neighbourhood branches in each state.

### **Move 13: Resample catastrophes on branch**

In this move, we sample a proposal from the prior distribution on catastrophes along a randomly chosen branch. When  $\rho$  is fixed, the prior distribution on the number of catastrophes on branch  $i$  is  $\text{Poisson}(\rho\Delta_i)$ . When  $\rho$  is unknown and integrated out with respect to its Gamma prior, the prior distribution on catastrophe counts on branches is Negative Multinomial, and Negative Binomial on a single branch.

1. Select a branch  $i$  with probability  $\Delta_i/\Delta$
2. Sample new catastrophe count  $n'_i$  from the prior on branch  $i$
3. Sample new relative locations  $u'_1, \dots, u'_{n'_i} \stackrel{i.i.d.}{\sim} U(0, 1)$
4. Form the proposed state  $C'$  from by removing the catastrophes on  $i$  from  $C$  and adding  $(i, u'_1), \dots, (i, u'_{n'_i})$ .

When coupling this move, we sample the target branches and new catastrophe counts from maximal couplings of their respective distributions. We sample new catastrophe locations from a maximal coupling. Let  $n'_{X,i_X}$  denote the proposed catastrophe count on the target branch in state  $X$ , and  $n'_{Y,i_Y}$  likewise for  $Y$ . In the proposed state,  $n'_{X,i_X} \wedge n'_{Y,i_Y}$  catastrophes will have locations in common, with the remainder sampled independently.

This procedure for coupling proposed catastrophe locations is equivalent to simulating a dominating catastrophe process and maximally coupling the random thinning operation to obtain the proposed catastrophes for  $X$  and  $Y$ . For example, if the prior on catastrophes is a Poisson process with rate  $\rho$ , then we could simulate a Poisson process with rate  $\rho(\Delta_{i_X} \vee \Delta_{i_Y})$  on  $[0, 1]$ , and include each point as a relative location for a catastrophe on  $i_X$  in  $X$  with probability  $\Delta_{i_X}/(\Delta_{i_X} \vee \Delta_{i_Y})$ , and likewise for  $Y$  (Kingman, 1992). If we sample from a maximal coupling at each candidate point, then  $n'_{X,i_X} \sim \text{Poisson}(\rho\Delta_{i_X})$  and  $n'_{Y,i_Y}$  likewise, and  $X$  and  $Y$  will have  $n'_{X,i_X} \wedge n'_{Y,i_Y}$  relative locations in common.

### **Move 14: resample catastrophe locations on branch**

In this move, we sample a catastrophe at random from those on the tree, and propose a new location along its branch. We only apply this move when fitting the lateral transfer model, and it fails if there are no catastrophes on the tree.

1. Select branch  $i$  with probability  $n_i/n$
2. Select a catastrophe  $(i, u)$  uniformly at random from those on  $i$
3. Sample a new relative location  $u' \sim U(0, 1)$
4. Form the proposed state  $C' \leftarrow C \cup \{(i, u')\} \setminus \{(i, u)\}$ .

As with moves 11 and 12, we sample the target branches from a maximal coupling of their distributions, and we sample a catastrophe identified by its location from a maximal coupling of discrete Uniform distributions. We propose the same location  $u'$  to both states  $X$  and  $Y$ .

### C.5 Moves 15–19: Stochastic Dollo model parameters

For all of these proposals, we sample  $\eta \sim U(1/2, 2)$  and use it to rescale the parameter. The move fails if the proposal is outside its valid range.

#### Moves 15 & 16: rescale $\mu$ or $\beta$

We sample  $\nu$  as above and propose a new death rate  $\mu' \leftarrow \nu\mu$ . When coupling this move, we sample from a maximal coupling of  $U(\mu/2, 2/mu)$  for each state. The proposal for the lateral transfer rate  $\beta$  is identical.

#### Move 17: rescale $\kappa$

We typically fix  $\kappa$  for the reasons described in Appendix A, but if it is included in the model then we restrict it to a subset of  $[0, 1]$ . The scaling move fails if the proposed  $\kappa$  falls outside its range.

#### Moves 18 & 19: rescale missing data parameters

Under the SD model, the true presence/absence status of a trait is recorded at leaf  $i$  with probability  $\xi_i$ , and  $\Xi = (\xi_i)_{i \in L}$ . To update a single parameter (move 18), we

- Select a leaf  $i \sim U(L)$
- Propose  $\xi'_i \leftarrow 1 - \nu(1 - \xi)$ .

To couple this move, we select the same  $i$  for both states  $X$  and  $Y$ , and sample the proposed missingness parameter from a maximal coupling of the corresponding Uniform distributions.

We propose to update all of the missingness parameters (move 19) using the same  $\nu$  term. As with rescaling multiple node times by a common factor (moves 7–9), we cannot sample from a maximal coupling, so instead we use the same  $\nu$  to make proposals in both state  $X$  and  $Y$ .